J. Micropalaeontology, 43, 93–119, 2024
https://doi.org/10.5194/jm-43-93-2024

Journal of Micropalaeontology
Open Access

Diatom and radiolarian biostratigraphy in the Pliocene sequence of ODP Site 697 (Jane Basin, Atlantic sector of the Southern Ocean)

Yuji Kato[1,a], **Iván Hernández-Almeida**[2], **and Lara F. Pérez**[3]

[1]Faculty of Life and Environmental Sciences, University of Tsukuba, Tennodai, Tsukuba, Ibaraki, 305-8572, Japan
[2]ETH Zürich, Geological Institute, Department of Earth Science, Zurich, Switzerland
[3]Geological Survey of Denmark and Greenland, Aarhus University City 81, building 1872, 6 floor, DK-8000 Aarhus C, Denmark
[a]present address: Marine Core Research Institute, Kochi University, Monobe, Nankoku, Kochi, 783-8502, Japan

Correspondence: Yuji Kato (yuji.kato@kochi-u.ac.jp)

Received: 16 June 2023 – Revised: 5 February 2024 – Accepted: 19 March 2024 – Published: 17 May 2024

Abstract. Bio- and magnetostratigraphic events are essential to construct age models of marine sedimentary sequences for which no other dating methods are available. In this study, we re-visit Ocean Drilling Program (ODP) Leg 113, Hole 697B (drilled in the Jane Basin, the Atlantic sector of the Southern Ocean; 61°48.626′S, 40°17.749′W), to refine diatom and radiolarian biostratigraphy for the early and middle Pliocene, a warm interval of Earth's history which is often considered a climatic analogue for the future. In total, 16 bioevents were identified in the diatom analysis and 3 in the radiolarian analysis. From these, 8 diatom events and one radiolarian event were identified for the first time in Hole 697B. We correlate the identified bioevents with existing paleomagnetic datums in Hole 697B to recalculate and update the ages of the bioevents. Although most of the calculated ages fall within the range of previously published ages, this study allowed us to narrow the age ranges of a number of bioevents. The updated biostratigraphy, as well as the assemblage data presented here, contributes to strengthening the Pliocene chronological framework at Hole 697B for future paleoceanographic work. In addition, we found an interval characterized by abundant reworked Miocene microfossils (e.g., *Denticulopsis* spp.) at ca. 4.5–3.7 Ma that may suggest sediment disturbance caused by regional tectonic and/or paleoceanographic events in the Southern Ocean during this time interval.

1 Introduction

Biostratigraphic events are essential to construct age models for paleoceanographic reconstructions that are key to understand past and future climate change. In polar regions, calcareous microfossils (e.g., foraminifera and calcareous nannofossils) are usually not well preserved, except for time-limited warm events (e.g., Saavedra-Pellitero et al., 2017) or geological periods with different tectonic and oceanographic configurations and/or ocean biogeochemistry (e.g., Mutterlose and Wise, 1990; Pospichal and Wise, 1990; Berggren, 1992a, b). In contrast, siliceous microfossils (diatoms and radiolarians) are abundant and generally well preserved in polar regions from both hemispheres during most of the Cenozoic. To some extent, the chronostratigraphic framework of the Southern Ocean and, thus, our understanding of paleoenvironmental changes are as good as our understanding of the siliceous microfossils preserved in the sediments.

The siliceous microfossil stratigraphy and associated paleoceanographic studies in the Southern Ocean have been developed through coring expeditions over the past few decades (e.g., Ramsay and Baldauf, 1999; Scherer et al., 2007). Based on their recovery and outputs, sediments drilled during the Ocean Drilling Program (ODP) Leg 113 show potential for further analyses. This expedition was a pioneer in the drilling of the Weddell Sea (the Atlantic sector of the

Southern Ocean), providing insight into the reconstruction of the history of sea ice and Antarctic bottom-water formation and the understanding of global ocean circulation and climate change during the Cenozoic (Burckle et al., 1990; Kennett and Barker, 1990). The recovered sediment sequences are important to paleoclimatologists because they cover the Pliocene, a climate period with pCO_2 levels similar or higher than those observed today and are therefore relevant for developing paleoceanographic studies.

Initial age interpretations for ODP Leg 113, Hole 697B, drill cores were based on low-resolution biostratigraphy (ca. 9.5 m sample intervals) and magnetostratigraphy (Gersonde and Burckle, 1990; Gersonde et al., 1990; Lazarus, 1990). However, in general, published bioevent ages often have large uncertainties or are regionally asynchronous, which limit the constraint on ages of newly obtained core samples (e.g., Cody et al., 2008). Recalculation of biostratigraphic datums based on recent paleomagnetic timescales (Ogg, 2020) and the microfossil analysis based on the latest taxonomic schemes (e.g., Yanagisawa and Akiba, 1990; Jordan and Priddle, 1991; Harwood and Maruyama, 1992; Gersonde and Bárcena, 1998; Sjunneskog et al., 2012) may also contribute to the refinement of biostratigraphic ages in Hole 697B and aid in determining the isochrony and/or diachrony of bioevent ages.

In this study, we conducted microfossil analyses with higher-resolution sampling to refine the biostratigraphy of the early and middle Pliocene (ca. 4.5–3.1 Ma) section of Hole 697B. In addition, we correlated the bioevents with magnetostratigraphy in the same core (Table 1; Shipboard Scientific Party, 1988) with reference to the recent geomagnetic timescale (Ogg, 2020) to constrain bioevent age ranges. This is essential for reliable paleoceanographic reconstructions and further Southern Ocean paleoclimate research.

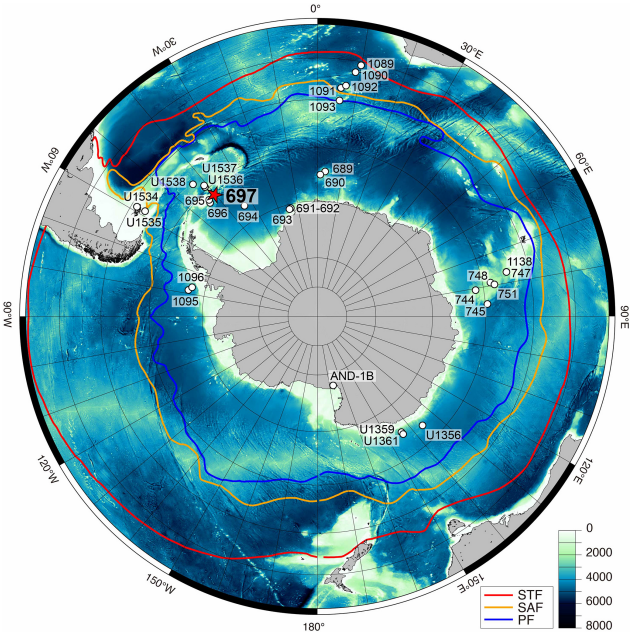

Figure 1. Location of ODP Leg 113, Hole 697B (focus of this study), and related drilling sites in the Southern Ocean on ETOPO1 bathymetry map (Amante and Eakins, 2009). Oceanographic fronts are from Orsi et al. (1995), showing the Subtropical Front (STF; red line), Subantarctic Front (SAF; yellow line), and Polar Front (PF; blue line).

2 Materials and methods

Hole 697B was drilled in the Jane Basin, Weddell Sea, in the Atlantic sector of the Southern Ocean (61°48.626′S, 40°17.749′W; Fig. 1). The 24 samples selected for the analyses were taken between 113-697B-25X-2, 85–86 cm (246.825 m below sea floor or m b.s.f.), and 113-697B-13X-2, 85–86 cm (130.955 m b.s.f.), with an average sampling resolution of ca. 5 m (i.e., two samples per core), doubling the existing resolution from previous studies (Gersonde and Burckle, 1990; Gersonde et al., 1990; Lazarus, 1990). The lithology of the upper part of the analyzed interval (ca. 160–130 m b.s.f.) is diatom-bearing clay mud, whereas the lower part of the interval (ca. 250–160 m b.s.f.) is formed by clay (Shipboard Scientific Party, 1988).

For diatom analysis, approximately 30 mg of freeze-dried sample was mixed with ∼ 4 mL of hydrogen peroxide (H_2O_2; 30 %) in a 15 mL polypropylene conical centrifuge tube to remove organic matter. The tube was boiled in a constant-temperature bath at 70 °C for 1–2 h. After boiling, the tube was filled with Milli-Q water and allowed to stand for 8 h. The residue was separated by decanting off the chemical water. The decanting process was repeated five times. Microslides for light microscopic observation of diatoms were prepared subsequently. The sample was suspended in Milli-Q water, from which 600 µL was extracted with a pipette and put on an 18 × 18 mm cover glass previously cleaned with acetone (C_3H_6O) to evenly distribute suspended particles, dried on a hot plate at 50–60 °C, and mounted on a slide glass using Pleurax. The counting method for fossil diatom valves follows that of Akiba (1986). A single valve of a centric diatom was counted as one when greater than a half of a whole valve was observed. Broken specimens of pennate diatoms were counted as one valve when both apices were observed, and those only with the other side of apex were counted as 0.5 valves and later converted to a number of valves. At least 200 diatom valves were counted at the species level for each sample. After counting, the entire area of the cover glass was scanned to check if there were any species missed in the original tally. The absolute abundance of diatoms (diatom valves per 1 g sediment) was also calculated for each sample based on the weight of mounted sample, the scanned area (scanned length × diameter of a field of view), and the number of counted diatom valves. In other words, the absolute abundance of diatoms was calcu-

lated based on the following equation.

$$\text{Diatom abundance} = \frac{\#\text{diatoms counted} \times \text{cover glass area}\,(\text{mm}^2)}{\text{scanned area}\,(\text{mm}^2) \times \text{picked sample}\,(\text{mL})} \times \frac{\text{sample suspension}\,(\text{mL})}{\text{sediment mass}\,(\text{g})}$$

The preservation of diatoms was determined qualitatively and recorded following the classification of Iwai and Winter (2002); G is for good (slight to no fragmentation and dissolution), M is for moderate (moderate fragmentation and dissolution), and P is for poor (severe effects of fragmentation and dissolution).

For radiolarian analysis, 5 cc samples were freeze-dried, weighed, washed, and wet sieved through a 63 µm mesh. The residue $>$ 63 µm was transferred to a 10 mL vial and filled up to 6 mL with distilled water. Slide preparation follows the method described by Tetard et al. (2020) but using a modified version of 3D-printed decanters to use 24 × 24 mm cover slips. Radiolarian analyses were made using a Zeiss Axioscope light microscope with ×400 to ×600 magnification. Since radiolarian fossils in the samples were less abundant than diatoms, the presence or absence of biostratigraphic marker species was recorded instead of the census of the whole assemblage.

The observed bioevents were correlated and recalculated with the magnetostratigraphy obtained from the site to provide updated ages of early and middle Pliocene bioevents. It should be noted that although several works presented paleomagnetic reversal datums at Site 697, there are differences in the interpretation of these paleomagnetic events (Shipboard Scientific Party, 1988; Pudsey, 1990). We therefore revisited the paleomagnetic data presented in the initial site report (Fig. 21 in Shipboard Scientific Party, 1988) to determine which interpretation should be adopted in the current study. Ages of these paleomagnetic reversal datums were updated using the Ogg (2020) timescale (Table 1).

3 Results and discussion

3.1 Paleomagnetic interpretation in Hole 697B

Main differences in the paleomagnetic interpretations at Site 697 concern the depth interval of C3n (ca. 250–200 m b.s.f.), which corresponds to the lower part of the analyzed interval in the current study (Shipboard Scientific Party, 1988; Pudsey, 1990). According to the age–depth model proposed by the Shipboard Scientific Party (1988), the interval ca. 235.2 to 201 m b.s.f. would correspond to C3n.1n, whereas C3n.2n would be located at ca. 261 to 247.2 m b.s.f. (Fig. 2). On the other hand, Pudsey (1990) identified C3n.1n in the ca. 207.5–201 m b.s.f. interval and C3n.3n at ca. 261.0 to 247 m b.s.f., whereas chrons C3n.1r, C3n.2n, and C3n.2r were not clearly identified. The difference between the two interpretations

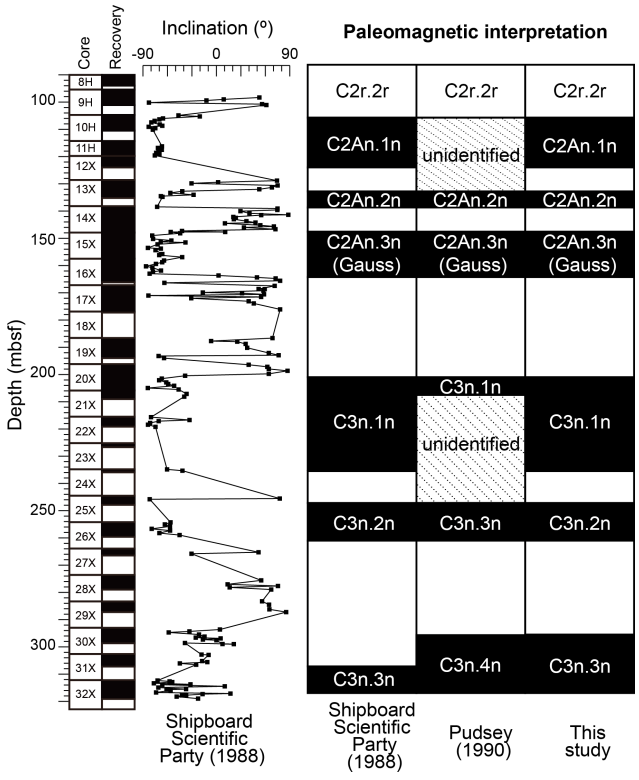

Figure 2. Paleomagnetic interpretation at Hole 697B. Magnetostratigraphic data are after Fig. 22 in Shipboard Scientific Party (1988).

seems to be due to the Shipboard Scientific Party's (1988) interpretation of the small shift in the inclination values at ca. 210–200 m b.s.f. as a fluctuation, but it was interpreted as C3n.1r by Pudsey (1990) (Fig. 2).

Because this discrepancy was not resolved in subsequent studies, and for the ease of our biostratigraphic analysis, we revised this paleomagnetic interpretation. According to the paleomagnetic data (i.e., Fig. 22 in Shipboard Scientific Party, 1988), the magnitude of the shift in the ca. 210–200 m b.s.f. interval is obviously smaller than that of other paleomagnetic reversal events (Fig. 2). Therefore, we adopt the interpretation of the Shipboard Scientific Party (1988) in this study and assign a depth of 235.2 m b.s.f. to the base of C3n.1n (Fig. 2; Table 1). The top of C3n.1n chron was assigned to 201.0 m b.s.f., which agrees with both Shipboard Scientific Party (1988) and Pudsey (1990). In addition, the base of the C2An.1n chron was assigned to 124.0 m b.s.f. based on paleomagnetic data by Shipboard Scientific Party (1988), although this chron lies outside of the interval analyzed in this study. For the top of C3n.3n (base of C3n.2r), we assigned a depth of 295.7 m b.s.f., where a large negative shift in the inclination values occurred, adopting the interpretation of Pudsey (1990).

Table 1. Paleomagnetic datums at Hole 697B. Event depths are after the compilation (see text) of Pudsey (1990) and Shipboard Scientific Party (1988). The ages are updated using the recent geomagnetic timescale by Ogg (2020).

Event	Event depth (m b.s.f.)	Age (Ma)
C2An.1n, top	105.7	2.595
C2An.1n, base	124.0	3.032
C2An.2n, top	132.8	3.116
C2An.2n, base	138.7	3.207
C2An.3n, top	147.6	3.330
C2An.3n, base	164.25	3.596
C3n.1n, top	201.0	4.187
C3n.1n, base	235.2	4.300
C3n.2n, top	247.2	4.493
C3n.2n, base	261.0	4.631

3.2 Diatom biozones and datum events

Most of the diatom specimens were fragmented, with the preservation of intervals noted as poor to moderate across the studied interval (Table 2). Diatom preservation was poor between 201.06 to 153.3 and 246.8 to 235.6 m b.s.f., and the absolute abundance of diatoms was also remarkably low, except for Core 113-697B-19X (ca. 190 m b.s.f.) (Fig. 3). The relative abundance of weakly silicified taxa such as *Fragilariopsis* spp. was low, whereas heavily silicified *Stephanopyxis* spp. and needle-shaped diatoms (*Thalassiothrix* spp. and *Thalassionema* spp.) showed higher abundances (Fig. 3). Therefore, the original assemblage composition may have been partially affected by dissolution. The upper part of the analyzed interval (152.3 to 131.0 m b.s.f.) showed better preservation and higher absolute diatom abundance (on the order of 10^6–10^7 valves g^{-1}), which is consistent with the initial description in the shipboard report (Shipboard Scientific Party, 1988). The diatom assemblages in the upper part of the analyzed interval included higher proportions of *Rouxia* spp. and *Chaetoceros* spp., while other taxa with more fragile valves such as *Fragilariopsis* spp. also occurred at a relative abundance of a few percent (Fig. 3).

A total of 90 diatom taxa and 16 diatom bioevents (i.e., first occurrence, FO, and last occurrence, LO) were observed in the analyzed interval (Fig. 4). Photomicrographs of selected diatom taxa are also shown in Fig. 5. Among these bioevents, five are reported for the first time at Hole 697B. The stratigraphic distribution of the taxa is shown in Table 2. The higher-resolution sampling of this study compared to that of Gersonde and Burckle (1990) enabled a more detailed description of biohorizons in Hole 697B. The details of the biostratigraphic zones and other significant bioevents identified within the early to middle Pliocene interval of the ODP Hole 697B core are presented below, mainly applying the diatom zonation of Zielinski and Gersonde (2002). In Table 3, we present previously published bioevent ages during the Pliocene from various sites in the Southern Ocean (Gersonde and Burckle, 1990; Gersonde et al., 1990; Baldauf and Barron, 1991; Harwood and Maruyama, 1992; Harwood et al., 1992; Zielinski and Gersonde, 2002; Winter and Iwai, 2002; Iwai et al., 2002; Bohaty et al., 2003; Cody et al., 2008, 2012; Tauxe et al., 2012; Winter et al., 2012; Florindo et al., 2013). Note that the previously published ages shown in Table 3 are modified values based on the latest geomagnetic timescale by Ogg (2020). As for Cody et al. (2008), we cited the ages of the Average Range Model that incorporate assumptions about incompleteness in the fossil record. Similarly, for Cody et al. (2012), we cited the Hybrid Range Model ages that also incorporate assumptions about reworking of diatoms along the Antarctic continental margin sediments.

Thalassiosira inura Zone

Author: Gersonde and Burckle (1990), revised by Baldauf and Barron (1991)

Top: FO of *Fragilariopsis barronii*

Base: FO of *Thalassiosira inura*

Remarks: The FO of *Fragilariopsis barronii*, which forms the top of this biozone, was observed at 207.505 m b.s.f. (113-697B-21X-1, 85–86 cm/21X-2, 85–86 cm). The observation is consistent with Gersonde and Burcke (1990), who reported the lowest occurrence of this species within Core 113-697B-21X. The calculated age (4.21 Ma) is in agreement with the age ranges from other Southern Ocean sites (4.6–4.2 Ma; Table 3). *Thalassiosira inura*, whose FO event defines the base of this zone, showed continuous occurrences at Hole 697B (Figs. 3 and 4). The taxon also occurred in the lowermost sample in this study (Core 113-697B-25X-2W, 82–83 cm; 246.825 m b.s.f.; Table 2). Therefore, the age of the FO event for this taxon was considered to be, at least, older than ca. 4.5 Ma, which is consistent with the range of published ages (6.3–4.2 Ma; Table 3). Most studies have settled on an age range of ca. 4.9–4.5 Ma for this event (e.g., Gersonde and Burckle, 1990; Winter and Iwai, 2002, in ODP Site 1096; Cody et al., 2008, 2012; Tauxe et al., 2012), while some studies have reported older ages of ca. 5.6–5.3 Ma (Baldauf and Barron, 1991; Harwood and Maruyama, 1992; Winter and Iwai, 2002, in ODP Site 1095) (Table 3). There is no regional trend in the previously published ages, and the cause of the asynchronies is currently unknown.

In addition, we observed continuous occurrence of *Fragilariopsis praeinterfrigidaria*, and the lowermost occurrence of the taxon was between Samples 113-697B-25X-1, 85–86 cm, and 25X-2, 82–83 cm (246.09 m b.s.f., Fig. 4). The calculated age of this horizon corresponds to 4.48 Ma (Table 2). We tentatively assigned this horizon to a FO event of the taxon. However, the obtained age of this event at Site 697 should be used with caution as only one sample was examined below it. The obtained age lies within the published age ranges, although a large range of ages has been published

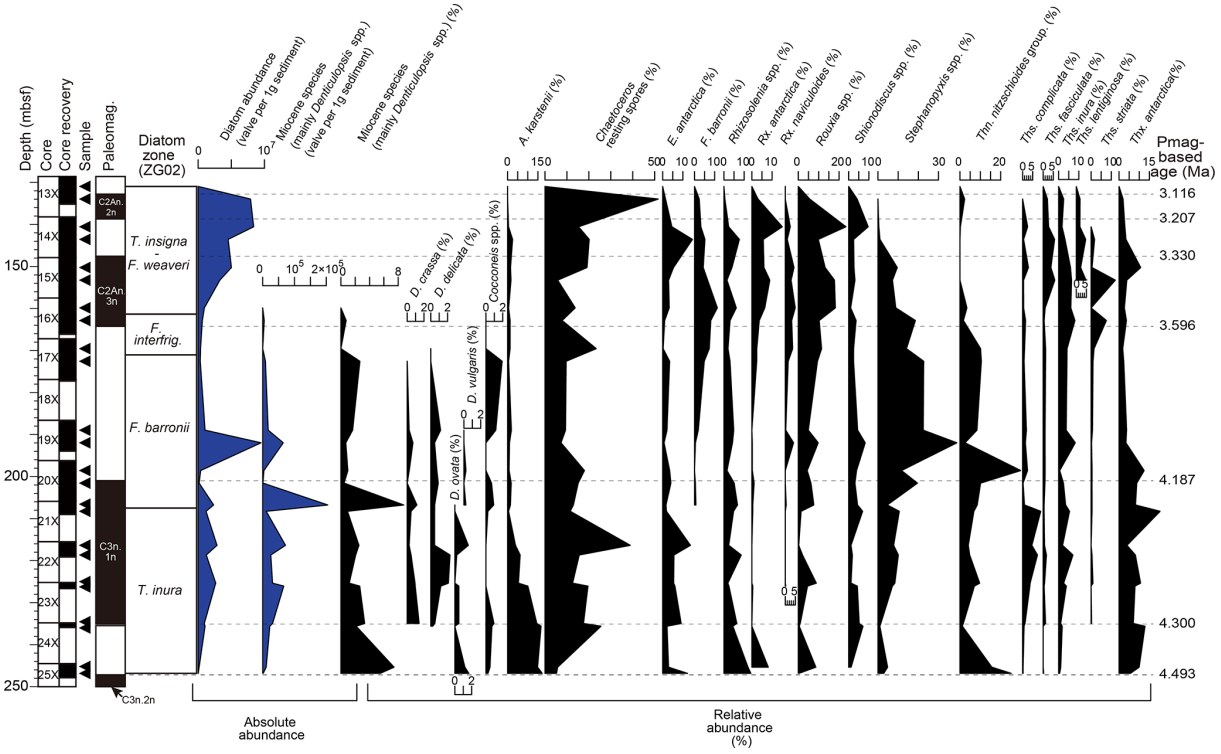

Figure 3. Stratigraphic abundance distribution of selected diatoms in Hole 697B. The right panel shows the relative abundance (%) of the major taxa of the assemblages. The left panel shows the absolute abundance (valve per 1 g sediment) of total diatoms and a typical Miocene taxon (*Denticulopsis* spp. (excluding *D. delicata*) and *N. denticuloides*).

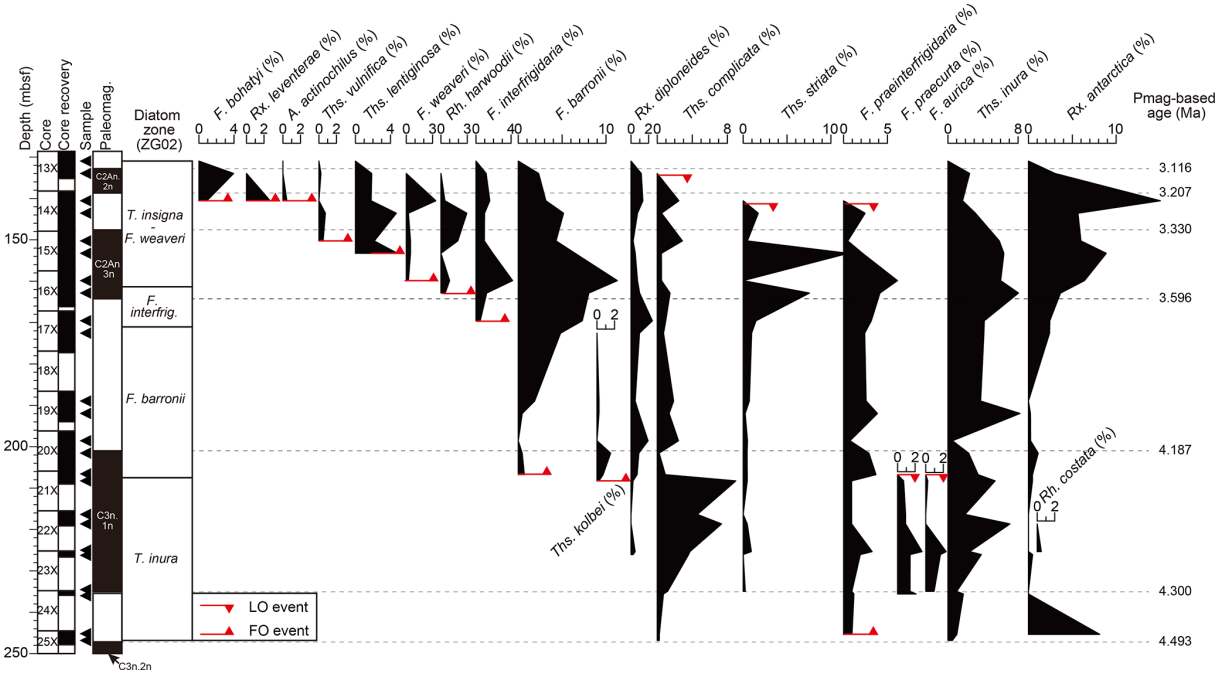

Figure 4. Relative abundance of biostratigraphic marker diatoms observed in this study.

Table 2. Stratigraphic occurrences of diatom species from ODP Leg 113, Hole 697B.

Diatom zone, after Zielinski and Gersonde (2002)	Sample	Mid depth (m b.s.f.)	Pmag-based age (Ma)	Preser-vation	*Actinocyclus actinochilus*	*Actinocyclus curvatulus*	*Actinocyclus ingens*	*Actinocyclus karstenii*	*Actinocyclus maccollumii*	*Actinocyclus octonarius*	*Actinocyclus* spp.	*Azpeitia tabularis*	*Chaetoceros* resting spore	*Cocconeis californica*	*Cocconeis costata*	*Cocconeis fasciolata*	*Cocconeis* spp.	*Corethron pennatum*	*Coscinodiscus asteromphalus*
T. insigna–F. weaveri	113-697B-13X-2, 85–86 cm	130.955	3.10	M	0.5	0	0.5	0.5	0	0	0	0	141	0	0	0	0	0	0
	113-697B-13X-4, 85–86 cm	133.955	3.13	P	0	0	2	0	0.5	0	0	1	111	0	0	0	0	0	0
	113-697B-14X-2, 85–86 cm	140.555	3.23	M	1	1	0	1	1.5	0	0	0	34	0	0	0	0	0	0
	113-697B-14X-4, 85–86 cm	143.555	3.27	M	0	0	1	5	2	0	0	0	41	0	0	0	0	0	0
	113-697B-15X-2, 85–86 cm	150.255	3.37	M	0	1	1	3	5	0	0	0	40	0	0	0	0	0	0
	113-697B-15X-4, 85–86 cm	153.255	3.42	P	0	1.5	0	3.5	3.5	0	0	0	12	0	0	0	0	0	1
	113-697B-16X-2, 85–86 cm	159.855	3.53	P	0	1	0	1	1	0	0	0	28	0	0	0	0	0	0
F. interfrig.	113-697B-16X-4, 85–86 cm	162.855	3.57	P	0	0	0	2.5	0.5	0	0	0	16	0	0	0	1	0	0
	113-697B-17X-2, 85–86 cm	169.555	3.68	P	0	0	0	2.5	0	0	0	0	48	0	0	0	0	0	0
F. barronii	113-697B-17X-4, 85–86 cm	172.555	3.73	P	0	0	3	1	1	0	1	0	20	1	1.5	1.5	0	0	0
	113-697B-19X-2, 85–86 cm	188.955	3.99	P	0	0	2	4	0	0	0	0	20	0	2	0	0.5	0	0
	113-697B-19X-4, 85–86 cm	191.955	4.04	P	0	0	0	2	0	0	0	0	16	0	0	0	0	0	0
	113-697B-20X-2, 85–86 cm	198.555	4.15	P	0	1	1	1.5	0	0	0	0.5	37	0	0	0	0	0	0
	113-697B-20X-4, 85–86 cm	201.555	4.19	P	0	0.5	1	4	0	0	0	0	34	0	0.5	1	0	0	1
	113-697B-21X-1, 85–86 cm	206.755	4.21	M	0	1	2	3	0	4	0	1	28	0	1	1	0	0	0
T. inura	113-697B-21X-2, 85–86 cm	208.255	4.21	P	0	2	1	1	0	4	0	0	25	0	0.5	0	0	0	0
	113-697B-22X-1, 85–86 cm	216.355	4.24	M	0	0	1	8.5	0	0	0	0	85	0	0	0	0	0	1
	113-697B-22X-3, 15–16 cm	218.655	4.25	M	0	0	1.5	13.5	0	1	0	1	34	0	0	0	0	0	1.5
	113-697B-23X-1, 15–16 cm	225.355	4.27	M	0	1	0	11.5	0	1.5	0	0	27	0	0	0	0	0	1
	113-697B-23X-1, 85–86 cm	226.055	4.27	M	0	0.5	0	21	0	2	0	0	41	0	0	0	0	0	0
	113-697B-24X-1, 15–16 cm	234.955	4.30	M	0	0	5.5	30.5	0	4.5	0	0	37	1	1	0	0	0	0
	113-697B-24X-1, 79–80 cm	235.595	4.31	P	0	0	0	35	0	5	0	0	54	0	1.5	0	0	0	1
	113-697B-25X-1, 85–86 cm	245.355	4.46	P	0	0	6	31	0	0	0	0	12	0	0	1	0	1	0
	113-697B-25X-2, 82–83 cm	246.825	4.49	P	0	0	1.5	36	0	2	0	1	11	0	0.5	0	0	0	0.5

Table 2. Continued.

Diatom zone, after Zielinski and Gersonde (2002)	Sample	Mid depth (m b.s.f.)	Pmag-based age (Ma)	*Coscinodiscus marginatus*	*Coscinodiscus radiatus*	*Denticulopsis crassa*	*Denticulopsis delicata*	*Denticulopsis dimorpha*	*Denticulopsis dimorpha* var. *areolata*	*Denticulopsis hyalina*	*Denticulopsis ovata*	*Denticulopsis praedimorpha*	*Denticulopsis simonsenii*	*Denticulopsis vulgaris*	*Denticulopsis* spp.	*Eucampia antarctica*	*Fragilariopsis arcula*	*Fragilariopsis aurica*
T. insigna–F. weaveri	113-697B-13X-2, 85–86 cm	130.955	3.10	0	0	0	0	0	0	0	0	0	0	0	0	1	0	0
	113-697B-13X-4, 85–86 cm	133.955	3.13	0	0	0	0	0	0	0	0	0	0	0	0	3	0	0
	113-697B-14X-2, 85–86 cm	140.555	3.23	0	0	0	0	0	0	0	0	0	0	0	0	10	0	0
	113-697B-14X-4, 85–86 cm	143.555	3.27	0	0	0	0	0	0	0	0	0	0	0	0	29.5	0	0
	113-697B-15X-2, 85–86 cm	150.255	3.37	0	0	0	0	0	0	0	0	0	0	0	0	11	0	0
	113-697B-15X-4, 85–86 cm	153.255	3.42	0	0	0	0	0	0	0	0	0	0	0	0	6	0	0
	113-697B-16X-2, 85–86 cm	159.855	3.53	0	0	0	0	0	1	0	0	0	0	0	0	6.5	0	0
F. interfrig.	113-697B-16X-4, 85–86 cm	162.855	3.57	0	0	0	0	1	0	0	0	0	0	0	0.5	2	0	0
	113-697B-17X-2, 85–86 cm	169.555	3.68	0	0	0	0.5	0	0	0	0	0	0	0	0	0.5	0	0
F. barronii	113-697B-17X-4, 85–86 cm	172.555	3.73	0	1	1	0	0	0	0	0	0	1	0	3.5	7	0	0
	113-697B-19X-2, 85–86 cm	188.955	3.99	0	0	0.5	2.5	0	0	0	0	0	0	0.5	2.5	4.5	0	0
	113-697B-19X-4, 85–86 cm	191.955	4.04	0	0	1.5	1	0	0	0	0	0	0	0	0	1.5	0	0
	113-697B-20X-2, 85–86 cm	198.555	4.15	1	0	0.5	1.5	0	0	0	0	1	0	0.5	0	7	0	0
	113-697B-20X-4, 85–86 cm	201.555	4.19	0	3	0	2	0	0	0	0	0	0	0	1	9	0	0
	113-697B-21X-1, 85–86 cm	206.755	4.21	2.5	0	2.5	1	2	3	0	7	1	1	0.5	2	3.5	0	2.5
T. inura	113-697B-21X-2, 85–86 cm	208.255	4.21	2	0.5	1	1	0	0	0	0	0	0	0	1	4	0	0.5
	113-697B-22X-1, 85–86 cm	216.355	4.24	0	0	0.5	1	0	0	0	3.5	0	0	0	1.5	29.5	0	0
	113-697B-22X-3, 15–16 cm	218.655	4.25	0	0	1	5	1	0	1	0.5	0	0	0	1	12	1	0
	113-697B-23X-1, 15–16 cm	225.355	4.27	0	4	2	4.5	0	0	0	0	0	0	0	0.5	11.5	0	5
	113-697B-23X-1, 85–86 cm	226.055	4.27	0	1.5	2	2.5	0	0	0	1	0	1	0	1.5	12.5	0	3.5
	113-697B-24X-1, 15–16 cm	234.955	4.30	0	1.5	3	1	1	0	0	1	0	1	0	1	19	0	2
	113-697B-24X-1, 79–80 cm	235.595	4.31	0	0.5	0	0.5	0	1	0	0	0	0	0	3.5	4.5	0	0
	113-697B-25X-1, 85–86 cm	245.355	4.46	0	0	0	0	2.5	3	0	2.5	3	0	0	4.5	6	0	0
	113-697B-25X-2, 82–83 cm	246.825	4.49	0	0.5	0	0	1.5	2.5	0	3.5	2	0	0	0	25.5	0	0

Table 2. Continued.

Diatom zone, after Zielinski and Gersonde (2002)	Sample	Mid depth (m b.s.f.)	Pmag-based age (Ma)	*Fragilariopsis barronii*	*Fragilariopsis bohatyi*	*Fragilariopsis cylindrus*	*Fragilariopsis interfrigidaria*	*Fragilariopsis laqueata*	*Fragilariopsis oceanica*	*Fragilariopsis praecurta*	*Fragilariopsis praeinterfrigidaria*	*Fragilariopsis robusta*	*Fragilariopsis sublinearis*	*Fragilariopsis weaveri*	*Fragilariopsis* sp. A	*Fragilariopsis* spp.	*Grammatophora* spp.	*Hemidiscus cuneiformis*
T. insigna–F. weaveri	113-697B-13X-2, 85–86 cm	130.955	3.10	4.5	10.5	0	0.5	2	0	0	0	0.5	7	0	2.5	0	0	0
	113-697B-13X-4, 85–86 cm	133.955	3.13	5	8.5	0	2.5	0	0	0	0	0.5	4.5	4.5	7.5	0.5	0	0
	113-697B-14X-2, 85–86 cm	140.555	3.23	7	2	0	3.5	0	0	0	9	0	1.5	7.5	5	0	0	0
	113-697B-14X-4, 85–86 cm	143.555	3.27	10.5	0	0	2	0	0	0	5	0	1	0.5	0	0	0	0
	113-697B-15X-2, 85–86 cm	150.255	3.37	9	0	0	2	0	0	0	1	0	0	1	0.5	0	0	0
	113-697B-15X-4, 85–86 cm	153.255	3.42	13.5	0	0	4	0	0	0	4.5	0	0	1	1.5	0	0.5	0
	113-697B-16X-2, 85–86 cm	159.855	3.53	23	0	0	8.5	0	0	0	12.5	0	0	0.5	2.5	0	0	0
F. interfrig.	113-697B-16X-4, 85–86 cm	162.855	3.57	16.5	0	0	2.5	0	0	0	8.5	0	0	0	4	0	0	0
	113-697B-17X-2, 85–86 cm	169.555	3.68	15	0	0	1	0	0	0	6.5	0.5	0	0	4	0	0	0
F. barronii	113-697B-17X-4, 85–86 cm	172.555	3.73	10	0	0	0	0	1	0	5	0	0	0	2.5	0	0	0
	113-697B-19X-2, 85–86 cm	188.955	3.99	4	0	0.5	0	0	0	0	5.5	0	0	0	5.5	0	0	1
	113-697B-19X-4, 85–86 cm	191.955	4.04	1	0	0	0	0	0	0	8.5	0	0	0	5.5	0	0	0
	113-697B-20X-2, 85–86 cm	198.555	4.15	0	0	0	0	0	0	0	1.5	0	0	0	2.5	0	0	0
	113-697B-20X-4, 85–86 cm	201.555	4.19	1	0	0	0	0	0	0	6.5	1	0	0	2	0	0	0
	113-697B-21X-1, 85–86 cm	206.755	4.21	1.5	0	0	0	0	0	6.5	8	1	0	0	5	0	0	0
T. inura	113-697B-21X-2, 85–86 cm	208.255	4.21	0	0	0	0	0	0	1.5	2	0	0	0	0	0	0	0
	113-697B-22X-1, 85–86 cm	216.355	4.24	0	0	0.5	0	0	0	2	2	0	1	0	0	0	0	0.5
	113-697B-22X-3, 15–16 cm	218.655	4.25	0	0	0	0	0	0	2	2	0.5	0	0	0	1	0	0.5
	113-697B-23X-1, 15–16 cm	225.355	4.27	0	0	0	0	0	0	6	7	0	0	0	2	1	0	0
	113-697B-23X-1, 85–86 cm	226.055	4.27	0	0	1	0	0	0	3	4	0.5	0	0	1	0	0	0
	113-697B-24X-1, 15–16 cm	234.955	4.30	0	0	0.5	0	0	0	3	2	1	0	0	0.5	0	0	0
	113-697B-24X-1, 79–80 cm	235.595	4.31	0	0	0	0	0	0	4.5	2.5	0	0	0	0.5	0	0	0
	113-697B-25X-1, 85–86 cm	245.355	4.46	0	0	0	0	0	0	0	2	0	0	0	0	0	0	0
	113-697B-25X-2, 82–83 cm	246.825	4.49	0	0	0	0	0	0	0	0	0	0	0	0	1.5	0	0

Table 2. Continued.

Diatom zone, after Zielinski and Gersonde (2002)	Sample	Mid depth (m b.s.f.)	Pmag-based age (Ma)	*Hemidiscus karstenii*	*Nitzschia denticuloides*	*Paralia* spp.	*Proboscia alata*	*Proboscia barboi*	*Rhizosolenia antennata* f. *semispina*	*Rhizosolenia costata*	*Rhizosolenia crassa*	*Rhizosolenia harwoodii*	*Rhizosolenia polydactyla*	*Rhizosolenia* spp.	*Rouxia antarctica*	*Rouxia constricta*	*Rouxia diploneides*	*Rouxia heteropolara*
T. insigna–F. weaveri	113-697B-13X-2, 85–86 cm	130.955	3.10	0	0	0	0	0	0	0	0	0	0	1	5	0	1.5	0
	113-697B-13X-4, 85–86 cm	133.955	3.13	0	0	0	0	0	0	0	0	1	0	0	6.5	0	2.5	0
	113-697B-14X-2, 85–86 cm	140.555	3.23	0	0	0	1	0	0	0	0	1	0	4	33.5	0.5	3	0
	113-697B-14X-4, 85–86 cm	143.555	3.27	0	0	0	0	0	0	0	1	6	0	8	11.5	0	1.5	0.5
	113-697B-15X-2, 85–86 cm	150.255	3.37	1	0	0	0	0	0	0	0	4	0	4	12.5	0	0.5	0
	113-697B-15X-4, 85–86 cm	153.255	3.42	0	0	0	0	0	1	0	1	0	0	1	18.5	0	1	0
	113-697B-16X-2, 85–86 cm	159.855	3.53	1	0	0	0	0	0	0	1	2	0	9	13	0	1.5	0
F. interfrig.	113-697B-16X-4, 85–86 cm	162.855	3.57	0	0	0	0	0	0	0	0	1	0	5	7.5	0	2	2
	113-697B-17X-2, 85–86 cm	169.555	3.68	1	0	2	0	0	0	0	0	0	0	4	5	0	5	0
F. barronii	113-697B-17X-4, 85–86 cm	172.555	3.73	0	0	0	0	1	0	0	0	0	0	6	5	0	2	2
	113-697B-19X-2, 85–86 cm	188.955	3.99	0	0	0.5	0	1	0	0	0	0	1	9	0	0	1	2
	113-697B-19X-4, 85–86 cm	191.955	4.04	0	0	0	0	0	2	0	1	0	0	6	0.5	0	2	1
	113-697B-20X-2, 85–86 cm	198.555	4.15	0	0	+	0	3	1	0	0	0	1	1	0.5	0	4	1
	113-697B-20X-4, 85–86 cm	201.555	4.19	0	0	1.5	0	0	0	0	1	0	0	10	2.5	0	2	1
	113-697B-21X-1, 85–86 cm	206.755	4.21	1	0	0	0	0	2	0	0	0	0	12	1	0	1.5	4
T. inura	113-697B-21X-2, 85–86 cm	208.255	4.21	1	0	0	0	8	0	0	0	0	0	10	1	0	0.5	+
	113-697B-22X-1, 85–86 cm	216.355	4.24	0	0	0	0	1	0	0	0	0	0	5	0	0	0	0.5
	113-697B-22X-3, 15–16 cm	218.655	4.25	0	0	0	0	1	0	3	1	0	0	14	0	0	0	0.5
	113-697B-23X-1, 15–16 cm	225.355	4.27	1	0	0	0	6	0	1	0	0	0	3	0	0	1	8.5
	113-697B-23X-1, 85–86 cm	226.055	4.27	0	0	0	0	3	1	0	0	0	0	4	1	0	0.5	2
	113-697B-24X-1, 15–16 cm	234.955	4.30	1	0	0	0	4	0	0	0	0	0	13	0	0	0	+
	113-697B-24X-1, 79–80 cm	235.595	4.31	0	0	0	0	7	1	0	1	0	0	7	0	0	0	1
	113-697B-25X-1, 85–86 cm	245.355	4.46	0	0	0	0	9	1	0	7	0	0	16	17	0	0	0
	113-697B-25X-2, 82–83 cm	246.825	4.49	0	2	3	0	5	0	0	1	0	0	26	0	0	0	0.5

Table 2. Continued.

Diatom zone, after Zielinski and Gersonde (2002)	Sample	Mid depth (m b.s.f.)	Pmag-based age (Ma)	*Rouxia isopolica*	*Rouxia leventerae*	*Rouxia naviculoides*	*Rouxia* spp.	*Shionodiscus oestrupii*	*Shionodiscus tetraoestrupii*	*Stellarima microtrias*	*Stephanopyxis* spp.	*Synedropsis* spp.	*Thalassionema nitzschioides* group	*Thalassiosira complicata*	*Thalassiosira convexa* var. *aspinosa*	*Thalassiosira fasciculata*	*Thalassiosira frenguelliii*	*Thalassiosira gravida*
T. insigna–F. weaveri	113-697B-13X-2, 85–86 cm	130.955	3.10	0.5	0	1	4	1	1	1	0	0	2	0	0	1	0.5	0
	113-697B-13X-4, 85–86 cm	133.955	3.13	0.5	0.5	0	2	5	4	1	1	0.5	5	1.5	0	4.5	1	0
	113-697B-14X-2, 85–86 cm	140.555	3.23	1	6	5.5	2.5	5	16.5	2	1	0	0.5	5.5	0	6	0	0
	113-697B-14X-4, 85–86 cm	143.555	3.27	0.5	0	2	4	0.5	4.5	3.5	2	0	0	1	0	11.5	0	0
	113-697B-15X-2, 85–86 cm	150.255	3.37	1	0	9	4.5	1	4.5	3.5	20	0	0	6	1	8	0	0
	113-697B-15X-4, 85–86 cm	153.255	3.42	2	0	6	9.5	1	5.5	4.5	15	0	0	1	4	12	0	0
	113-697B-16X-2, 85–86 cm	159.855	3.53	2	0	10	10.5	0	2	0	18	0	7	1	0	2	0	1
F. interfrig.	113-697B-16X-4, 85–86 cm	162.855	3.57	0	0	6.5	3	7	0.5	2	38	3	3.5	3	0	1	0	0
	113-697B-17X-2, 85–86 cm	169.555	3.68	1	0	7.5	5	5	0	1.5	29	2	21	2	0	2.5	0	0
F. barronii	113-697B-17X-4, 85–86 cm	172.555	3.73	1	0	3	6.5	4	1	3.5	47	0	22	1.5	0	2.5	0	0
	113-697B-19X-2, 85–86 cm	188.955	3.99	0.5	0	0.5	6.5	5.5	4	4	48	0	18	4	1	2	0	0
	113-697B-19X-4, 85–86 cm	191.955	4.04	2	0	9	7	10	8	1.5	86	0	5.5	3	0	2	0	0
	113-697B-20X-2, 85–86 cm	198.555	4.15	1.5	0	0	2	6	2	1.5	24	0	62	5	0	2	0	0
	113-697B-20X-4, 85–86 cm	201.555	4.19	1	0	0	7.5	5.5	1.5	6	44	0	23	0.5	1	2	0	0
	113-697B-21X-1, 85–86 cm	206.755	4.21	2	0	1	7	6	3.5	4	10	0	18.5	2	0	1	0	1
T. inura	113-697B-21X-2, 85–86 cm	208.255	4.21	+	0	0	1.5	11	4	0.5	23	0	15	19.5	0	1	0	0
	113-697B-22X-1, 85–86 cm	216.355	4.24	+	0	0	0	2.5	0	3	17	0	9	10	0	1.5	0	0
	113-697B-22X-3, 15–16 cm	218.655	4.25	3.5	0	0	0.5	2	2	3.5	22	0	10.5	16	0	3.5	0	0
	113-697B-23X-1, 15–16 cm	225.355	4.27	3.5	0	0	6	2.5	0	2.5	18	0	21	8	0	1.5	0	0
	113-697B-23X-1, 85–86 cm	226.055	4.27	1.5	0	0.5	4	7	2	5	15	0	15	7.5	0	1	0	0
	113-697B-24X-1, 15–16 cm	234.955	4.30	0	0	0	2	11	0	4	3	0	3.5	2.5	0	2.5	0	0
	113-697B-24X-1, 79–80 cm	235.595	4.31	0	0	0	0	11.5	3.5	2	2	0	2.5	1.5	0	0	0	0
	113-697B-25X-1, 85–86 cm	245.355	4.46	0	0	0	1	2	0.5	2	10	0	33	0.5	0	0	0	0
	113-697B-25X-2, 82–83 cm	246.825	4.49	0	0	0	0	0	0	1	6	0	53.5	0.5	0	0.5	0	0

Table 2. Continued.

Diatom zone, after Zielinski and Gersonde (2002)	Sample	Mid depth (m b.s.f.)	Pmag-based age (Ma)	*Thalassiosira inura*	*Thalassiosira kolbei*	*Thalassiosira lentiginosa*	*Thalassiosira oliverana*	*Thalassiosira ritscheri*	*Thalassiosira scotia*	*Thalassiosira striata*	*Thalassiosira torokina*	*Thalassiosira tumida*	*Thalassiosira vulnifica*	*Thalassiosira* spp.	*Thalassiothrix antarctica*	*Thalassiothrix miocenica*	*Triceratium* spp.	*Trichotoxon reinboldii*
T. insigna–F. weaveri	113-697B-13X-2, 85–86 cm	130.955	3.10	1	0	4.5	0	0	6	0	1	0	0.5	4	2.5	0	0	0
	113-697B-13X-4, 85–86 cm	133.955	3.13	5	0	4	1	0	2	0	1	1	0.5	7	4	0	0	0.5
	113-697B-14X-2, 85–86 cm	140.555	3.23	3.5	0	4	0.5	2	0	5	1	3.5	0	16.5	6	0	0	0
	113-697B-14X-4, 85–86 cm	143.555	3.27	6	0	9.5	0	1	1	3.5	1	1	1.5	13.5	6.5	0	0	0
	113-697B-15X-2, 85–86 cm	150.255	3.37	11.5	0	4.5	0.5	0	1	1	3	1.5	1	8	21	0	0	0
	113-697B-15X-4, 85–86 cm	153.255	3.42	12.5	0	10	0	0	0	25	1	1	0	16	7.5	0	0	0
	113-697B-16X-2, 85–86 cm	159.855	3.53	11.5	0	0	1.5	0	2	0	0	0	0	8	5	0	0	0
F. interfrig.	113-697B-16X-4, 85–86 cm	162.855	3.57	15.5	0	0	4	0	4.5	15.5	1.5	0	0	13.5	7	0	0	0
	113-697B-17X-2, 85–86 cm	169.555	3.68	8	0	0	0	0	0	3	0.5	0	0	13.5	3.5	0	0	0
F. barronii	113-697B-17X-4, 85–86 cm	172.555	3.73	8	0.5	0	0	0	4	2	1	0	0	11.5	4.5	0	0	0
	113-697B-19X-2, 85–86 cm	188.955	3.99	7.5	0.5	0	0	0	8	1.5	0	0	0	18	7.5	0.5	0	0
	113-697B-19X-4, 85–86 cm	191.955	4.04	17	0.5	0	2	0	2	0.5	1	0	0	5	7	1.5	0	0
	113-697B-20X-2, 85–86 cm	198.555	4.15	1	0	0	0	0	0	1	0	0	0	3	24	0	0	+
	113-697B-20X-4, 85–86 cm	201.555	4.19	5	3.5	0	2	0	0	1	0	0	0	11.5	18.5	0	0	0
	113-697B-21X-1, 85–86 cm	206.755	4.21	7	1.5	0	1	0	4	1	0	1	0	12	16.5	0	0	0
T. inura	113-697B-21X-2, 85–86 cm	208.255	4.21	11	0.5	0	4	0	0	1	1	0	0	11	41.5	2	0	1
	113-697B-22X-1, 85–86 cm	216.355	4.24	4	0	0	0	0	0	0	1	0	0	14.5	8	0	0	0
	113-697B-22X-3, 15–16 cm	218.655	4.25	14.5	0	0	6.5	0	0	1	1	0	0	11.5	16.5	0	0	0
	113-697B-23X-1, 15–16 cm	225.355	4.27	5	0	0	1	0	0	2	1.5	0	0	9.5	21.5	0.5	0	0
	113-697B-23X-1, 85–86 cm	226.055	4.27	7.5	0	0	1.5	0	0	0	0	0	0	12.5	15.5	0.5	0	0
	113-697B-24X-1, 15–16 cm	234.955	4.30	2	0	0	8	0	3	0.5	2.5	0	0	15.5	14	0	0	0
	113-697B-24X-1, 79–80 cm	235.595	4.31	3.5	0	0	4	0	0	0	5	0	0	18.5	25.5	0	0	0
	113-697B-25X-1, 85–86 cm	245.355	4.46	2	0	0	1	0	0	0	3	0	0	8	19.5	0	1	0
	113-697B-25X-2, 82–83 cm	246.825	4.49	1	0	0	0.5	0	0	0	1	0	0	7.5	11	0	0	0

Table 2. Continued.

Diatom zone, after Zielinski and Gersonde (2002)	Sample	Mid depth (m b.s.f.)	Pmag-based age (Ma)	Indet	Total valves counted	Diatom abundance (valve g^{-1})	*Denticulopsis* spp. without *D. delicata* + *N. denticuloides* (valve g^{-1})
T. insigna–F. weaveri	113-697B-13X-2, 85–86 cm	130.955	3.10	3.5	213.5	2.5.E+07	0.0.E+00
	113-697B-13X-4, 85–86 cm	133.955	3.13	1.5	215	7.9.E+06	0.0.E+00
	113-697B-14X-2, 85–86 cm	140.555	3.23	2	222.5	8.4.E+06	0.0.E+00
	113-697B-14X-4, 85–86 cm	143.555	3.27	3.5	203.5	4.5.E+06	0.0.E+00
	113-697B-15X-2, 85–86 cm	150.255	3.37	1	209	5.0.E+06	0.0.E+00
	113-697B-15X-4, 85–86 cm	153.255	3.42	0	208.5	3.3.E+06	0.0.E+00
	113-697B-16X-2, 85–86 cm	159.855	3.53	9	203.5	9.4.E+05	4.6.E+03
F. interfrig.	113-697B-16X-4, 85–86 cm	162.855	3.57	3.5	205	6.4.E+05	4.7.E+03
	113-697B-17X-2, 85–86 cm	169.555	3.68	5	205.5	3.6.E+05	0.0.E+00
F. barronii	113-697B-17X-4, 85–86 cm	172.555	3.73	6	207.5	3.2.E+05	8.5.E+03
	113-697B-19X-2, 85–86 cm	188.955	3.99	6.5	214	1.0.E+06	1.7.E+04
	113-697B-19X-4, 85–86 cm	191.955	4.04	0	220	9.5.E+06	6.5.E+04
	113-697B-20X-2, 85–86 cm	198.555	4.15	3	206	3.8.E+05	3.7.E+03
	113-697B-20X-4, 85–86 cm	201.555	4.19	6	225	1.5.E+05	6.7.E+02
	113-697B-21X-1, 85–86 cm	206.755	4.21	3.5	216.5	2.3.E+06	2.1.E+05
T. inura	113-697B-21X-2, 85–86 cm	208.255	4.21	1.5	217.5	1.2.E+06	1.1.E+04
	113-697B-22X-1, 85–86 cm	216.355	4.24	4	218.5	2.8.E+06	7.2.E+04
	113-697B-22X-3, 15–16 cm	218.655	4.25	3	218	1.2.E+06	2.5.E+04
	113-697B-23X-1, 15–16 cm	225.355	4.27	5	215	2.7.E+06	3.1.E+04
	113-697B-23X-1, 85–86 cm	226.055	4.27	2.5	209.5	2.5.E+06	6.6.E+04
	113-697B-24X-1, 15–16 cm	234.955	4.30	2	211	9.3.E+05	3.1.E+04
	113-697B-24X-1, 79–80 cm	235.595	4.31	1	211.5	1.0.E+06	2.2.E+04
	113-697B-25X-1, 85–86 cm	245.355	4.46	1	209	1.5.E+05	1.1.E+04
	113-697B-25X-2, 82–83 cm	246.825	4.49	0.5	210	2.4.E+04	1.3.E+03

Table 3. Compilation of early Pliocene bioevents of diatoms and radiolarians (G is for Gersonde et al., 1990; GB is for Gersonde and Burckle, 1990; L90 is for Lazarus, 1990; BB is for Baldauf and Barron, 1991; Ca is for Caulet, 1991; F is for Florindo et al., 2013; H is for Harwood et al., 1992; HM is for Harwood and Maruyama, 1992; L92 is for Lazarus, 1992; ZG is for Zieliski and Gersonde, 2002; WI is for Winter and Iwai, 2002; I is for Iwai et al., 2002; L01 is for Lazarus, 2001; B is for Bohaty et al., 2003; VL is for Vigour and Lazarus, 2002; T is for Tauxe et al., 2012; W is for Winter et al., 2012; C08 is for Cody et al., 2008; C12 is for Cody et al., 2012). Published age values based on earlier geomagnetic timescales (e.g., Berggeren et al., 1985; Cande and Kent, 1995) are recalculated based on the latest paleomagnetic dating scale (Ogg, 2020). Bioevents shown in bold font are the ones used to define the biozones in the current study. The ages of Average Range Model correspond to Cody et al. (2008), and for the Hybrid Range Model to Cody et al. (2012).

				ODP Leg 113	ODP Leg 119		ODP Leg 120			ODP Leg 177					ODP Leg 178		ODP Leg 183	IODP exp. 318			AND-RILL		
		Event	Range of published age (Ma)	Sites 689, 690, 697	Site 745	Site 744	Site 747	Site 748	Site 751	Site 1089	Site 1090	Site 1091	Site 1092	Site 1093	Site 1095	Site 1096	Site 1138	Site U1356	Site U1359	Site U1361	AND-1B	multiple sites	AND-1B
Diatom	FO	*Ths. vulnifica*	3.40–2.99		3.2	3.40	3.2	3.2	3.2	–	–	–	–	–	3.38–3.15	3.06–3.02	–	–	–	3.15	–	3.18–3.12	3.01–2.99
	FO	*Ths. insigna*	3.6–2.82	–	–	–	3.4	3.2	3.6–3.41	–	–	–	–	–	–	2.82	–	–	–	3.25	–	3.36–3.14	–
	LO	*Ths. complicata*	3.5–2.43	–	–	–	3.5	3.0	3.2	2.88	2.96	-	3.31	3.31	–	–	–	–	–	–	–	3.44–3.36	2.45–2.43
	LO	*Ths. striata*	3.5–2.4	–	–	–	–	2.9	3.4	–	2.82	–	3.50	–	–	–	–	–	–	–	–	2.96–2.89	2.42–2.40
	LO	*F. praeinterfrigidaria*	3.72–2.97	–	–	2.98	3.7–3.6	3.5	3.7	–	–	–	–	–	–	3.72–3.70	3.7	–	–	–	–	3.49–3.45	2.97
	FO	*F. bohatyi*	3.2	–	–	–	–	–	–	–	–	–	–	–	–	–	–	–	–	–	3.2	–	–
	FO	*Rx. leventerae*	2.77–2	–	–	–	–	–	–	–	–	–	–	–	–	–	–	–	–	–	–	2.08–2	2.77
	FO	*Ac. actinochilus*	2.81–2.72	–	–	–	–	–	–	–	–	–	–	–	–	–	–	–	–	–	–	2.81–2.72	2.73
	FO	*Ths. vulnifica*	3.4–3	–	2.9–2.8	3.40	3.2	3.2	3.2	–	–	–	–	–	3.38–3.06	3.06–3.06	3.2	-	3-.15	3.15	–	3.18–3.12	3.00
	FO	*Ths. lentiginosa*	4.6–3.76	–	–	4.01	4.6	4.2	4.2	–	–	–	–	–	–	–	–	–	–	–	–	4.11–3.86	3.78–3.76
	FO	***F. weaveri***	3.55–3.01	–	3.4–3.2	–	3.5	–	3.4	–	3.43	3.01	3.40	3.50	–	–	3.4	–	–	3.53	–	3.55–3.51	–
	FO	*Rh. harwoodii*	3.58–3.56	–	–	–	–	–	–	–	–	–	–	–	–	–	–	–	–	–	–	–	3.58–3.56
	FO	***F. interfrigidaria***	4.21–3.7	3.8	3.8	4.13	3.7	3.8	4.0	–	3.81	–	3.75	–	3.87–3.84	4.10–4.03	3.8	–	–	–	4.21	4.19–3.93	3.87–3.85
	LO	*N. wisei*	3.94–3.7	–	–	–	–	3.7	3.7	–	–	–	–	–	–	–	–	–	–	–	–	3.94–3.73	–
	LO	*D. delicata*	4.54–4.42	–	–	–	–	–	–	–	–	–	–	–	–	–	–	–	–	–	–	–	4.54–4.42
	FO	*Ths. kolbei*	4.7–3.7	–	–	3.95	4.6–3.7	4.2	4.2	–	–	–	–	–	–	–	–	–	–	–	–	4.02–3.8	4.70–4.64
	FO	*N. wisei*	4.7–4.5	–	–	–	–	4.1	4.5	–	–	–	–	–	–	–	–	–	–	–	–	4.7–4.56	–
	LO	*F. praecurta*	4.6–4.19	–	–	–	4.6	–	–	–	–	–	–	–	–	–	–	–	–	–	–	4.28–4.19	–
	LO	*F. aurica*	4.6–3.12	–	–	–	4.6–3.7	4.0	4.2	–	3.37	–	3.12	–	–	–	–	–	–	–	–	4.35–4.21	–
	FO	***F. barronii***	4.6–4.2	4.6–4.5	4.3	4.40	4.6	8.9–4.2	4.2	–	–	–	–	–	4.29–4.23	4.48–4.45	4.6–4.2	–	4.4	4.4	–	4.52–4.28	4.4
	LO	*Rh. costata*	4.3–3.6	–	–	–	3.6	4.2	4.2	–	–	–	–	–	–	–	–	–	–	–	–	4.3–4.2	–
	LO	*F. arcula*	4.6–3.75	–	–	–	4.6	4.0	4.2	–	4.09	–	3.75?	–	–	–	–	–	–	–	–	4.49–4.29	–
	FO	*Rx. diploneides*	4.7–3.7	–	–	–	4.5–3.7	3.8	4.3	–	–	–	–	–	–	–	–	–	–	–	–	4.7–4.61	–
	FO	*Ths. striata*	4.73–3.5	–	–	–	–	3.5	4.5	–	–	–	–	–	4.29–4.23	-	4.5	–	–	–	–	4.64–4.3	4.73–4.67
	FO	*F. praeinterfrigidaria*	6.83–4.2	–	4.98	6.83	6.0–4.6	8.9–4.2	6.3–4.8	–	–	–	–	–	5.91–5.82	–	–	–	–	–	–	4.78–4.72	4.98
	FO	*Ths. fasciculata*	4.80–3.7	–	–	–	4.5–3.7	4.2	4.5	–	–	–	–	–	4.29–4.23	–	–	–	–	–	4.34	4.42–4.25	4.80–4.76
	FO	*Rx. heteropolara*	4.8–4.03	4.7	4.1–4.03	–	~4.7	4.2	4.8	–	–	–	–	–	–	–	–	–	–	–	–	4.73–4.68	
	FO	*Rx. antarctica*	5.40–4.43	–	–	5.40	–	–	–	–	–	–	–	–	–	–	–	–	–	–	–	4.57–4.43	4.95
	LO	*F. clementia*	4.555	–	–	–	–	–	–	–	–	–	–	–	–	–	–	–	4.555	–	–	–	–
	FO	*Ths. complicata*	5.16–4.64	4.7	–	–	–	–	4.8	–	–	–	–	–	5.16–5.10	–	4.7	–	4.675	–	–	4.71–4.64	4.96
	FO	*Ths. inura*	6.3–4.2	4.90	5.3–5.2	5.45	6.0–4.6	8.9–4.2	6.3–4.8	–	–	–	–	–	5.93–5.59	4.64–4.59	–	4.74	4.74	4.74	4.74	4.77–4.71	4.91
	FO	*Rh. costata*	4.74–4.58	–	–	–	–	–	–	–	–	–	–	–	–	–	–	–	–	–	–	4.74–4.58	–
			References	G, GB	BB	F	H, HM	H, HM	H, HM	ZG	ZG	ZG	ZG	ZG	WI, I	WI, I	B03	T	T	T	W	C08	C12
Radiol-arian	**LO**	***P. vema***	2.5–2.3	2.5	2.44–2.42	2.35	2.43	2.43	2.43	–	–	–	–	–	–	–	–	–	2.3	–	–	–	–
	LO	*L. p. titan*	4.0–3.45	3.6	3.55–3.45	3.53	~3.50	4.0	3.90	–	–	–	–	–	3.499	–	–	–	–	–	–	–	–
	LO	*Lam. coronata*	3.719–3.7	–	–	–	–	~3.7	~3.7	–	–	–	–	–	3.719	–	–	–	–	–	–	–	–
	FO	*E. pseudoinflatum*	4.43–4.2	–	4.43–4.38	–	–	–	–	–	–	–	–	–	–	–	–	–	4.2	4.2	–	–	–
	FO	***P. vema***	4.88–4.2	4.6	4.61–4.56	4.88	~4.6	–	~4.6	–	–	–	–	–	4.59	–	4.58	4.2	4.2	4.2	–	–	–
	FO	*L. p. titan*	5.12–5.02	–	5.12–5.02	–	–	–	–	–	–	–	–	–	–	–	–	–	–	–	–	–	–
			References	L90	Ca	F	L92	L92	L92	–	–	–	–	–	L01	–	VL02	T	T	T			

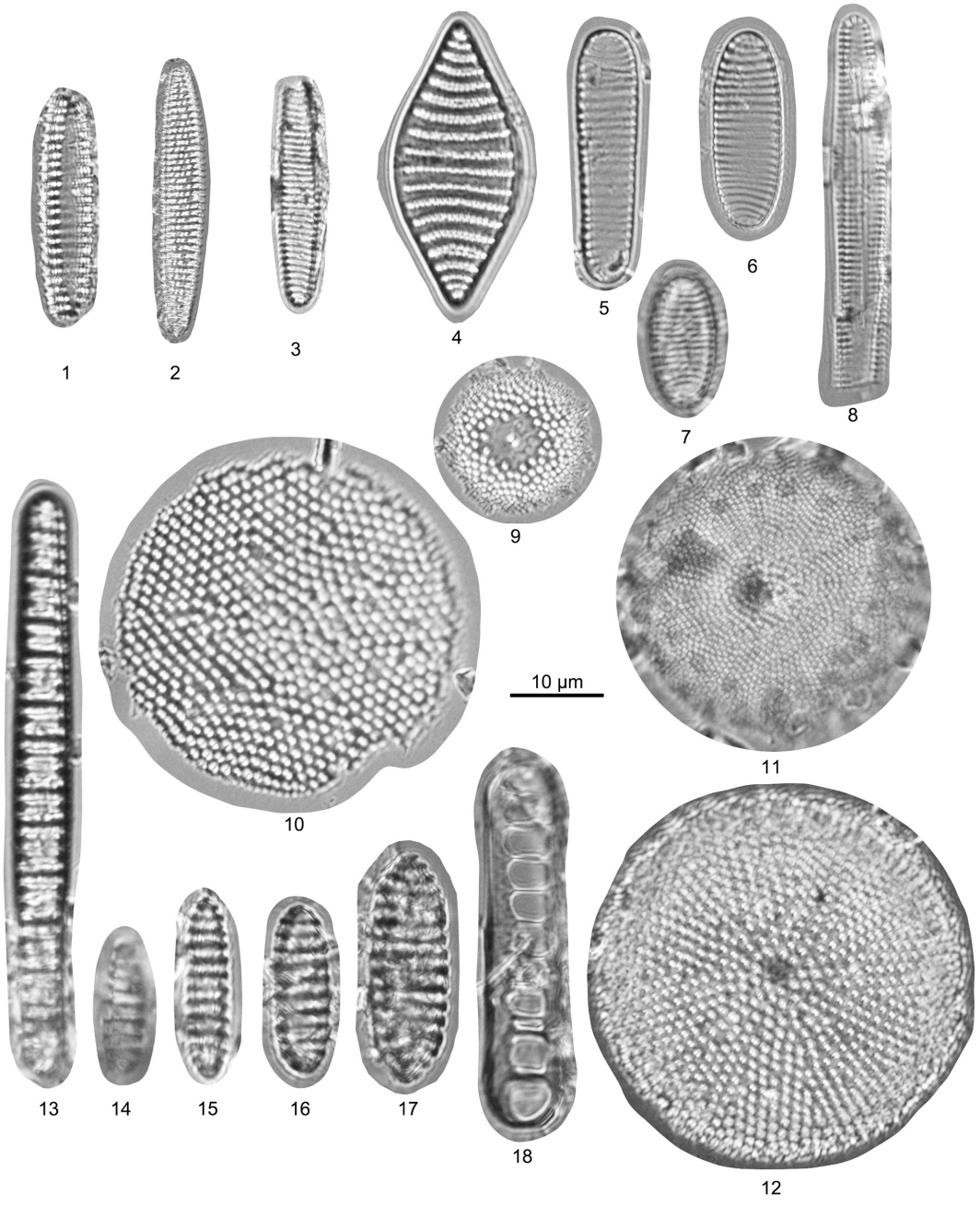

Figure 5. Photomicrographs of selected diatom species. **(1)** *Fragilariopsis weaveri* (697B-13X-4, 85–86 cm). **(2)** *Fragilariopsis praeinterfrigidaria* (697B-16X-2, 85–86 cm). **(3)** *Fragilariopsis interfrigidaria* (697B-13X-2, 85–86 cm). **(4)** *Fragilariopsis barronii* (697B-15X-4, 85–86 cm). **(5)** *Fragilariopsis* sp. A (697B-23X-1, 15–16 cm). **(6)** *Fragilariopsis praecurta* (697B-23X-1, 15–16 cm). **(7)** *Fragilariopsis aurica* (697B-24X-1, 15–16 cm). **(8)** *Rouxia diploneides* (697B-23X-1, 85–86 cm). **(9)** *Thalassiosira inura* (697B-16X-4, 85–86 cm). **(10)** *Thalassiosira striata* (697B-21X-1, 85–86 cm). **(11)** *Thalassiosira complicata* (697B-20X-2, 85–86 cm). **(12)** *Thalassiosira fasciculata* (697B-14X-4, 86–87 cm). **(13)** *Denticulopsis delicata* (697B-22X-3, 15–16 cm). **(14)** *Denticulopsis dimorpha* (697B-25X-1, 85–86 cm). **(15–16)** *Denticulopsis dimorpha* var. *areolata* (**15**: 697B-21X-1, 85–86 cm; **16**: 697B-24X-1, 79–80 cm). **(17–18)** *Denticulopsis ovata* (**17**: 697B-22X-1, 85–86 cm; **18**: 697B-25X-2, 82–83 cm).

for this event (Table 3). For example, Cody et al. (2008) presented an age of approximately 4.7 Ma. On the other hand, ages of ca. 4.9–4.2 Ma were proposed from the Indian Ocean sector (Baldauf and Barron, 1991; Harwood and Maruyama, 1992) and a somewhat older age of ca. 5.8 Ma from the Pacific Ocean sector (Winter and Iwai, 2002). The FO of *Thalassiosira kolbei* was found between Samples 113-697B-21X-2, 85–86 cm, and 22X-1, 85–86 cm (212.305 m b.s.f.;

Fig. 4). This bioevent has an age of ∼ 4 Ma, according to previous biostratigraphic works made in pelagic settings (Harwood and Maruyama, 1992; Cody et al., 2008; Florindo et al., 2013), while older ages between 4.7–4.6 Ma were found in near-shore settings in the Ross Sea (Winter et al., 2012) (Table 3). In this study, we obtained an age of 4.22 Ma, which falls within the range of previously published ages.

We also recognized occurrences of several stratigraphically important diatom taxa in this zone. The taxa that showed continuous occurrences included *Thalassiosira fasciculata*, *Thalassiosira complicata*, *Rouxia heteropolara*, and *Rouxia antarctica*. The lowermost occurrences of the former three taxa were observed in Sample 113-697B-25X-2, 82–83 cm (246.825 m b.s.f.), and that of the latter taxon was observed in Sample 113-697B-25X-1, 85–86 cm (245.355 m b.s.f.), which corresponds to an age of around 4.5 Ma (Table 2). Therefore, the FOs of these taxa should be older than ca. 4.5 Ma in Hole 697B. Note that the FO of *Thalassiosira complicata* has a wide range of published ages (e.g., 4.8–4.7 Ma in the Indian Ocean sector, Harwood and Maruyama, 1992; Bohaty et al., 2003; 5.16–5.10 Ma at ODP Site 1095 in the Pacific Ocean sector, Iwai and Winter, 2002; 4.675 Ma at International Ocean Drilling Program (IODP) Site U1359 in the Wilkes Land, Tauxe et al., 2012; Table 3).

In addition, other potentially important taxa, *Thalassiosira striata* and *Rouxia diploneides*, were found over a wide range of the analyzed interval, although sporadically; the lowermost occurrence was at samples 113-697B-24X-1, 15–16 cm (234.955 m b.s.f.), and 113-697B-23X-1, 85–86 cm (226.055 m b.s.f.), which corresponds to an age of around 4.3 Ma (Table 2). Therefore, the ages of the FOs for the taxa are likely to be older than ca. 4.3 Ma, which is also consistent with the published age ranges (4.73–3.5 Ma for FO of *Thalassiosira striata* and 4.7–3.7 Ma for FO of *Rouxia diploneides*; Table 3). In this biozone, the presence of *Rhizosolenia costata* and *Fragilariopsis arcula* was also recognized around 220 m b.s.f. (Table 2), which corresponds to ages of ca. 4.3–4.2 Ma. Although it was not possible to identify the biostratigraphic events for these taxa due to their sparseness in samples, the obtained fossil record does not contradict the existing published age ranges from various drilling sites (Table 3).

Fragilariopsis barronii Zone

Author: Weaver and Gombos (1981), renamed by Gersonde and Burckle (1990) and Zielinski and Gersonde (2002)

Top: FO of *Fragilariopsis interfrigidaria*

Base: FO of *Fragilariopsis barronii*

Recalculated age: 4.21–3.71 Ma

Remarks: The FO of *Fragilariopsis interfrigidaria*, which defines the top of the *Fragilariopsis barronii* zone, was observed between Samples 113-697B-17X-2, 85–86 cm, and 17X-4, 85–86 cm (171.055 m b.s.f.). We obtained an age of 3.71 Ma for the event, which is consistent with published ages (ca. 4.0–3.7 Ma; Gersonde and Burckle, 1990; Baldauf and Barron, 1991; Harwood and Maruyama, 1992; Zielinski and Gersonde, 2002; Winter and Iwai, 2002; Bohaty et al., 2003; Cody et al., 2012), although some studies reported slightly older ages (ca. 4.2–4.1 Ma; Winter et al., 2012; Florindo et al., 2013) (Table 3). The diatom assemblage found in the *Fragilariopsis barronii* zone at Hole 697B is mainly composed of *Chaetoceros* resting spores, *Stephanopyxis* spp., *Thalassionema nitzschioides*, *Thalassiosira inura*, and *Thalassiothrix antarctica*.

In addition, the following three bioevents were observed within the *Fragilariopsis barronii* zone. The LOs of *Fragilariopsis praecurta* and *Fragilariopsis aurica* were observed between samples 113-697B-20X-4, 85–86 cm, and 21X-1, 85–86 cm (204.155 m b.s.f.), for the first time at Hole 697B. The ages calculated in this study were 4.2 Ma. The age of LO of *Fragilariopsis praecurta* was in agreement with the few published ages for this event (i.e., 4.28–4.19 Ma; Cody et al., 2008) (Table 3). The LO of *Fragilariopsis aurica* also lay within the published age ranges (4.6–3.12 Ma; Table 3), although the range of published ages is as large as ca. 1.5 Myr. For example, ages of 4.6–3.7 Ma were presented in the Indian Ocean sector (ODP Sites 747, 748, and 751; Harwood and Maruyama, 1992), while younger ages of this event were reported in the Atlantic Ocean sector (e.g., 3.12 Ma at Site 1090 and 3.37 Ma at Site 1092; Zielinski and Gersonde, 2002; Table 3), which indicates a potential regional asynchrony in this event.

The uppermost occurrence of *Denticulopsis delicata* is observed at 180.755 m b.s.f. (113-697B-17X-4, 85–86 cm/113-697B-19X-2, 85–86 cm), and this species is reported in Hole 697B for the first time in this study, since it was only described slightly after the timing of the ODP Leg 113 expedition (Yanagisawa and Akiba, 1990). However, the correlation of this horizon with the magnetostratigraphy yielded an anomalously young age (3.86 Ma) when compared to the existing published age range of its LO event (4.54–4.42 Ma by the Hybrid Range Model of Cody et al., 2012). Considering that the uppermost occurrence of the taxon parallels that of other Miocene *Denticulopsis* species, the discrepancy in age values could be due to the transport of reworked sediments.

Fragilariopsis interfrigidaria Zone

Author: McCollum (1975), modified by Weaver and Gombos (1981) and Zielinski and Gersonde (2002)

Top: FO of *Fragilariopsis weaveri*

Base: FO of *Fragilariopsis interfrigidaria*

Recalculated age: 3.71–3.55 Ma

Remarks: The FO of *Fragilariopsis weaveri*, which defines the top of *Fragilariopsis interfrigidaria* Zone, was recognized for the first time in Hole 697B at 161.355 m b.s.f. (113-697B-16X-2, 85–86 cm/16X-4, 85–86 cm). The calculated age was 3.55 Ma (Table 2), which is in agreement with

the age range of ca. 3.5–3.4 Ma reported in studies from the Atlantic Ocean sector (Sites 1090, 1092, and 1093; Zielinski and Gersonde, 2002), the Indian Ocean sector (Sites 747 and 751, Harwood and Maruyama, 1992; Site 1138, Bohaty et al., 2003; Site U1361, Tauxe et al., 2012), and the Ross Sea shelf (Winter et al., 2012) (Table 3). However, younger age ranges for this event have been also reported from a part of the Atlantic Ocean sector (3.01 Ma at Site 1091; Zielinski and Gersonde, 2002; Table 3). We also observed the FO of *Rhizosolenia harwoodii* at 166.205 m b.s.f. (113-697B-16X-4, 85–86 cm/697B-17X-2, 85–86 cm). The event age calculated in this study (3.63 Ma) is consistent with the published age (3.58 to 3.56 Ma in Cody et al., 2012; Table 3), although there are only a limited number of reports on the age of this bioevent as this species was only described after ANDRILL (ANtarctic DRILLing Project) in the Ross Sea (Winter et al., 2012). The consistency of the event age obtained in this study with previous reports suggests the usefulness of this event as a biostratigraphic marker for Southern Ocean sediments.

Thalassiosira insigna–Fragilariopsis weaveri Zone

Author: Zielinski and Gersonde (2002)

Top: LO of *Thalassiosira insigna* (the event was not observed in this study)

Base: FO of *Fragilariopsis weaveri*

Remarks: The uppermost part of the analyzed interval (161.355–130.955 m b.s.f.) was defined as *Thalassiosira insigna–Fragilariopsis weaveri* Zone. The top of this zone is defined by the LO of *Thalassiosira insigna*, but this species was not present in the analyzed interval in this study. According to the initial report of Site 697 (Gersonde and Burckle, 1990), *Thalassiosira insigna* (listed as *Coscinodiscus insignis*) only occurred in Core 113-697B-12X-CC (ca. 125 m b.s.f.), and it was not reported in any other stratigraphic level. The reported age ranges for this event vary from site to site (3.6–2.82 Ma), although prior reports present the age of around 3.4–3.2 Ma (Table 3).

Within this biozone, the FO of *Fragilariopsis bohatyi* was observed at 142.055 m b.s.f. (113-697B-14X-2, 85–86 cm/14X-4, 85–86 cm) for the first time at Hole 697B. The age of the bioevent considering the geomagnetic polarity datum was recalculated as 3.25 Ma. Since this species is a recently described taxon (Sjunneskog et al., 2012), the only comparison available is an age of 3.2 Ma obtained from the analysis of the core from the western Ross Sea (Winter et al., 2012). The LO of *Thalassiosira striata* was observed at 137.255 m b.s.f. (113-697B-13X-2, 85–86 cm/113-697B-13X-4, 85–86 cm) for the first time at Hole 697B. This species is particularly abundant in Cores 113-697B-15X and 16X, with a calculated LO event age of 3.18 Ma (Table 2). The published age of the event ranges from 3.5 to 2.4 Ma (Table 3), and the specific ages include 2.4 Ma in the western Ross Sea (Cody et al., 2012), 2.9–3.4 Ma in the South Indian Ocean Sector (Sites 748 and 751; Harwood and Maruyama, 1992), and 3.5 Ma in the lower-latitudinal part of the Atlantic Ocean sector (Site 1092; Zielinski and Gersonde, 2002).

Other stratigraphically important diatom events were observed within this biozone. The LO of *Thalassiosira complicata* was observed at 132.455 m b.s.f. with a calculated age of 3.11 Ma (Table 2). Previously published ages range from 3.5 to 2.43 Ma (Harwood and Maruyama, 1992; Zielinski and Gersonde, 2002; Winter and Iwai, 2002), consistent with the obtained age value at Hole 697B. However, younger ages of $\sim$ 2.4 Ma have also been reported from near-shore settings (western Ross Sea; Winter et al., 2012; Cody et al., 2012). The FOs of *Rouxia leventerae* and *Actinocyclus actinochilus* were found at 142.055 m b.s.f. (113-697B-14X-2, 85–86 cm/14X-4, 85–86 cm) with calculated ages of 3.25 Ma. These bioevents have not been widely described in the literature (Cody et al., 2008, 2012), which are younger than those found in the current study (2.77–2 Ma for *Rouxia leventerae* and 2.81–2.72 Ma for *Actinocyclus actinochilus*; Table 3). Therefore, the age difference could be due to regional asynchronicity. The FO of *Thalassiosira vulnifica* was identified at 151.755 m b.s.f. (113-697B-15X-2, 85–86 cm/15X-4, 85–86 cm) (Fig. 4). The calculated age (3.40 Ma) falls within the range of previously published ages (3.4–3 Ma; Table 3). The FO of *Thalassiosira lentiginosa* was found at 156.555 m b.s.f. (113-697B-15X-4, 85–86 cm/16X-2, 85–86 cm) in this study, which is in agreement with the results of the initial reports (113-697B-15X-2, 48 cm/113-697B-15X-CC; 153.525 m b.s.f.; Gersonde and Burckle, 1990). The calculated age was 3.47 Ma, which is younger than other published ages from the Indian Ocean sector (ca. 4 Ma; Harwood and Maruyama, 1992; Florindo et al., 2013) and near-shore settings in the Ross Sea (3.8 Ma; Winter et al., 2012; Table 3). The LO of *Fragilariopsis praeinterfrigidaria* was observed in 113-697B-13X-4, 85–86 cm/113-697B-14X-2, 85–86 cm (137.255 m b.s.f.), with a calculated age of 3.18 Ma. The age obtained in this study agrees with previously published ages (2.97–3.72 Ma; Table 3), although the range of published ages is as large as ca. 0.7 Myr; e.g., ca. 3.7–3.0 Ma in the Indian Ocean sector (Baldauf and Barron, 1991; Harwood and Maruyama, 1992; Bohaty et al., 2003; Florindo et al., 2013), 2.97 Ma in the Ross Sea shelf (Cody et al., 2012), and 3.7 Ma in the Pacific Ocean sector (Site 1096; Winter and Iwai, 2002). In addition, the lowermost occurrence of *Thalassiosira ritscheri* found at 143.555 m b.s.f., which corresponds to an age of 3.27 Ma (Table 2), although the FO age of this taxon is not well established in previous studies.

3.3 Radiolarian biozones and datum events

In the radiolarian analysis, we observed nine relevant taxa and identified three bioevents in the analyzed interval (Fig. 6; Table 4). Photomicrographs of selected radiolarian taxa are shown in Fig. 7. Preservation of radiolarians was poor to moderate, except in samples from Core 113-697B-25X,

which was just poor. In fact, some samples (e.g., 113-697B-25X-2, 85–86 cm) yielded only a few fragmented specimens. The analyzed interval was categorized into two biozones, namely the Tau and Upsilon Zones, based on the radiolarian zonation by Lazarus (1992). Here we also present recalculated ages of the radiolarian events using geomagnetic timescales by Ogg (2020) and a comparison with previously published bioevent ages from various sites in the Southern Ocean (Lazarus, 1990, 1992, 2001; Caulet, 1991; Harwood et al., 1992; Vigour and Lazarus, 2002; Florindo et al., 2013; Table 3).

Tau Zone

Author: Lazarus (1992)

Top: FO of *Pseudocubus vema*

Base: LO of *Amphymenium challengerae* (the event was not observed in this study)

Remarks: We observed the FO of *Pseudocubus vema* between Samples 113-697B-24X-1, 85–86 cm, and 25X-1, 85–86 cm (240.475 m b.s.f.). This event defines the top of the Tau Zone. The calculated age obtained here (4.3 Ma) does not contradict previously proposed ages (4.88–4.2 Ma; Table 3). However, published ages vary by about 0.7 Myr. In addition, an occurrence of *Larcopyle polycantha titan* was recognized in Sample 113-697B-24X-1, 85–86 cm (235.595 m b.s.f.) (Table 4), which is consistent with the observation by Lazarus (1990), who also recognized the occurrence of the species between Cores 113-697B-23X and 24X (ca. 230 m b.s.f.). This was the only occurrence of this species in the current study, and we were not able to identify the LO or FO events for this taxon.

Upsilon Zone

Author: Lazarus (1992)

Top: LO of *Pseudocubus vema*

Base: FO of *Pseudocubus vema*

Remarks: Most of the analyzed interval was assigned to the Upsilon Zone. In this study, the uppermost occurrence of *Pseudocubus vema* was recognized at 137.255 m b.s.f. (113-697B-13X-4, 85–86 cm/113-697B-14X-2, 85–86 cm). Correlation with the magnetostratigraphy yielded an age of 3.18 Ma for this horizon (Table 4). This age is considerably older than previously published ages of 2.5–2.3 Ma (Table 3). In this study, only two samples were analyzed above this stratigraphic level, and the preservation of this core is not very good. Thus, the age of this LO event at Site 697 should be used with caution. Occurrence of *Larcopyle polycantha titan* was recognized only in one sample (113-697B-24X-1, 15–16 cm; 235.595 m b.s.f.), so it was not possible to identify its LO event (Fig. 6; Table 4). Nevertheless, this result is consistent with the initial observation by Shipboard Scientific Party (1988), who reported the uppermost occurrence of the species in Core 113-697B-24X. In addition, we did not find any specimen of *Cycladophora davisiana* from the analyzed interval (Cores 113-697B-13X to 25X), which is consistent with the observation by Shipboard Scientific Party (1988), who identified the FO of *Cycladophora davisiana* between 113-697B-12X-CC and 13X-CC. Therefore, subdivision of this biozone was not provided, as we did not find the bioevents that define the boundaries of the three subzones within the Upsilon Zone, i.e., LO *Larcopyle polycantha titan* (4.0–3.45 Ma, Lazarus, 1990, 1992, 2002; Caulet, 1991; Florindo et al., 2013) and the FO *Cycladophora davisiana* (2.7 Ma; Lazarus, 2002).

Other bioevents/occurrences observed within this interval included the LO of *Lampromitra coronata* at 190.455 m b.s.f. (113-697B-19X-2, 85–86 cm/113-697B-19X-4, 85–86 cm), which was recognized for the first time in Hole 697B. The event depth was in the lower part of the zone, which is consistent with the description by Lazarus (1992). A calculated age of 4.02 Ma was assigned for this datum in correlation with the geomagnetic timescale by Ogg (2020). The published age for this event is ca. 3.7 Ma (Lazarus, 1992, 2001) in the Indian Ocean and Atlantic Ocean sectors (Table 3). Thus, the obtained age here is lightly older than previously published ages. In addition, we observed sporadic occurrences of *Eucyrtidium pseudoinflatum*, even though the FO event could not be assigned. The lowermost occurrence of the taxon was at 206.755 m b.s.f. (113-697B-21X-1W, 85–86 cm), which corresponds to an age value of about 4.2 Ma (Table 4). This observation is consistent with previously published ages of the FO event for this taxon from the Indian Ocean sector (4.43–4.38 Ma; Caulet, 1991) and Wilkes Land (4.2 Ma; Tauxe et al., 2012).

3.4 Summary of the observed bioevents

We conducted micropaleontological analyses of the interval corresponding to early to middle Pliocene in Hole 697B and confirmed the occurrence of several Pliocene stratigraphic marker species, identifying 19 bioevents (16 diatom events and 3 radiolarian events) (Figs. 4 and 6). Figure 8 illustrates the ranges of previously published ages for the bioevents (listed in Table 3) against the biohorizons identified in this study. We recalculated and presented the age of each bioevent by correlating the biohorizons with the published magnetostratigraphy (Shipboard Scientific Party, 1988; Ogg, 2020). As a result, large ranges on the bioevent ages have been narrowed in this study (Fig. 9; Table 5).

Most of the bioevent ages calculated in this study lay within the age ranges proposed in previous studies (Fig. 8; Table 3). Among the observed taxa, *Fragilariopsis bohatyi* and *Rhizosolenia harwoodii* are the taxa that have been described recently (Sjunneskog et al., 2012; Winter et al., 2012), and the number of reported bioevent ages used to be quite limited (Cody et al., 2012; Winter et al., 2012). Therefore, the results obtained in this study can be fundamental data for future verification of the usefulness as stratigraphic

Table 4. Stratigraphic occurrences of selected radiolarian species from ODP Leg 113, Hole 697B.

Radiolarian zone, after Lazarus (1992)	Sample	Mid-depth (m b.s.f.)	Pmag-based (Ma) age	*Cycladophora pliocenica*	*Desmospyris spongiosa*	*Eucyrtidium calvertense*	*Eucyrtidium pseudoinflatum*	*Desmospyris rhodospyroides*	*Lampromitra coronata*	*Larcopyle polycantha titan*	*Pseudocubus vema*	*Siphonosphaera vesuvius*
Upsilon	113-697B-13X-2, 85–86 cm	130.955	3.10									
	113-697B-13X-4, 85–86 cm	133.955	3.13									
	113-697B-14X-2, 85–86 cm	140.555	3.23	x	x		?				x	
	113-697B-14X-4, 85–86 cm	143.555	3.27		x						x	
	113-697B-15X-2, 85–86 cm	150.255	3.37	x	x						x	
	113-697B-15X-4, 85–86 cm	153.255	3.42	x			x	x			x	
	113-697B-16X-2, 85–86 cm	159.855	3.53								x	
	113-697B-16X-4, 85–86 cm	162.855	3.57	x	x							
	113-697B-17X-2, 85–86 cm	169.555	3.68	x	x							
	113-697B-17X-4, 85–86 cm	172.555	3.73		x							
	113-697B-19X-2, 85–86 cm	188.955	3.99					x				
	113-697B-19X-4, 85–86 cm	191.955	4.04		x				x		x	
	113-697B-20X-2, 85–86 cm	198.555	4.15	x	x	x		x				
	113-697B-20X-4, 85–86 cm	201.555	4.19	x	x	x			x			
	113-697B-21X-1, 85–86 cm	206.755	4.21	x	x	x	?	x				x
	113-697B-21X-2, 85–86 cm	208.255	4.21	x	x	x			x		x	
	113-697B-22X-1, 85–86 cm	216.355	4.24	x	x				x		x	
	113-697B-22X-3, 15–16 cm	218.655	4.25	x	x				x		x	
	113-697B-23X-1, 15–16 cm	225.35	4.27	x	x				x			
	113-697B-23X-1, 85–86 cm	226.05	4.27	x	x				x		x	
	113-697B-24X-1, 15–16 cm	234.955	4.30	x							x	
	113-697B-24X-1, 85–86 cm	235.595	4.31	x	x					x	x	
Tau	113-697B-25X-1, 85–86 cm	245.355	4.46									
	113-697B-25X-2, 85–86 cm	246.825	4.49		?							

markers or isochrony of these bioevents. In addition, nine bioevents were identified and reported for the first time in Hole 697B: LO of *Thalassiosira striata* (3.18 Ma), FO of *Fragilariopsis bohatyi* (3.25 Ma), FO of *Rouxia leventerae* (3.25 Ma), FO of *Actinocyclus actinochilus* (3.25 Ma), FO of *Thalassiosira vulnifica* (3.40 Ma), FO of *Fragilariopsis weaveri* (3.55 Ma), FO of *Rhizosolenia harwoodii* (3.63 Ma), FO of *Thalassiosira kolbei* (4.22 Ma), and LO of *Lampromitra coronata* (4.02 Ma).

Bioevents with large regional differences in published age values (by about 0.5 million years or more) included the following: FO of *Thalassiosira inura* (6.3–4.2 Ma), FO of *Fragilariopsis praeinterfrigidaria* (6.83–4.2 Ma), FO of *Thalassiosira complicata* (5.16–4.64 Ma), FO of *Fragilariopsis barronii* (4.6–4.2 Ma), LO of *Fragilariopsis aurica* (4.6–3.12 Ma), FO of *Fragilariopsis interfrigidaria* (4.21–3.7 Ma), FO of *Thalassiosira kolbei* (4.7–3.7 Ma), LO of *Fragilariopsis praeinterfrigidaria* (3.72–2.97 Ma), LO of *Thalassiosira striata* (3.5–2.4 Ma), LO of *Thalassiosira complicata* (3.5–2.43 Ma), and FO of *Pseudocubus vema* (4.88–4.2 Ma) (Fig. 8; Table 3). Such regional differences in the bioevent ages could be due not only to differences in the actual timing of extinction/appearance by region or setting but also to truncation of the fossil records due to poor preservation of fossils or reworking. However, we were unable to determine the cause of the asynchrony in these events. In general, the number of hiatuses and reworking events in the Southern Ocean complicates the assignment of precise ages for bioevents.

In three events, the age values calculated in this study deviated significantly from the age ranges proposed by previous studies: FO of *Thalassiosira lentiginosa* (3.53–3.42 Ma in this study, while 4.6–3.76 Ma in previous studies), LO of *Lampromitra coronata* (4.04–3.99 Ma in this study; ca. 3.7 Ma in previous studies), and LO of *Pseudocubus vema* (3.23–3.14 Ma in this study, while 2.5–2.3 Ma in previous re-

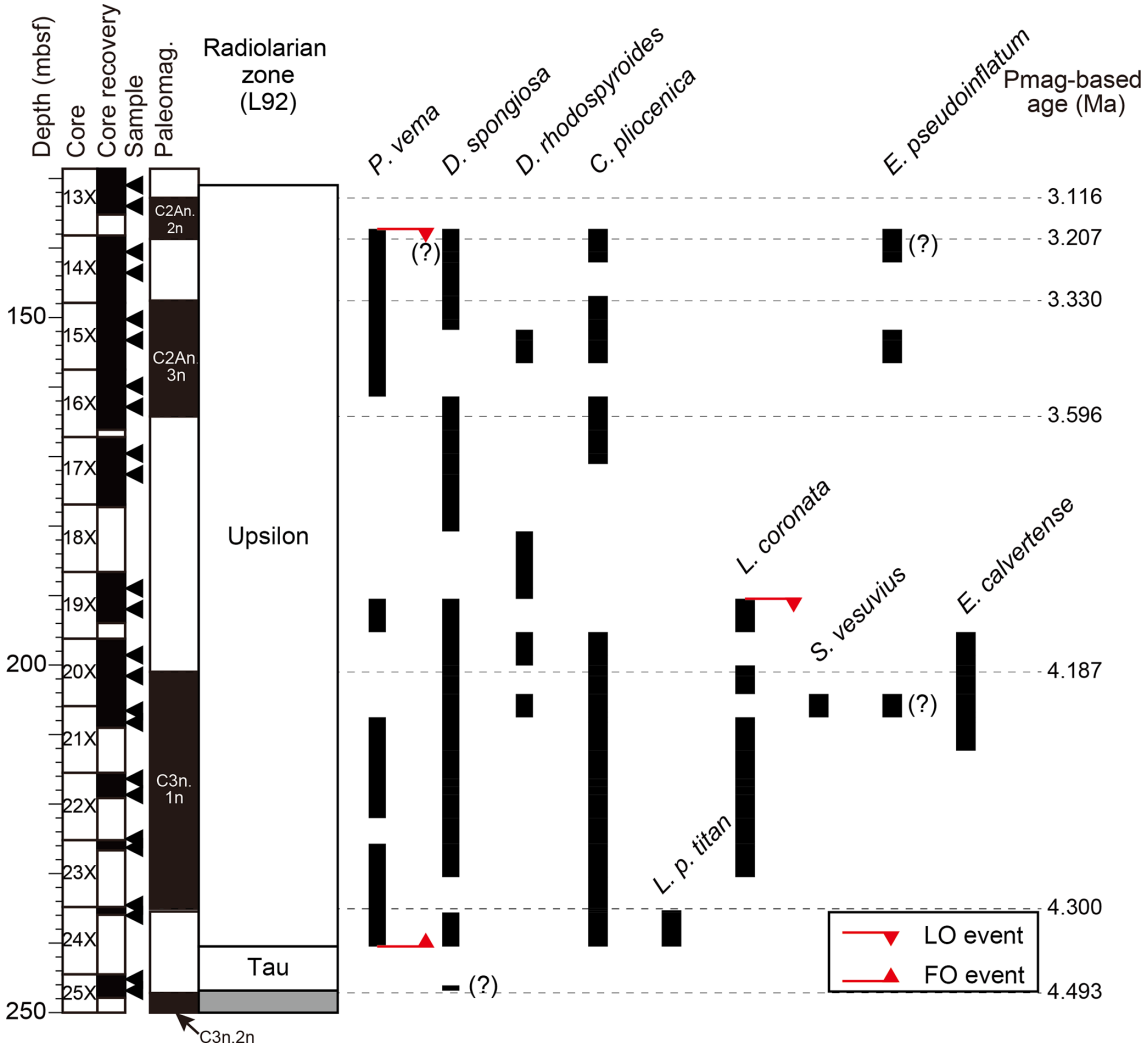

Figure 6. Range chart of the biostratigraphic marker radiolarians observed in this study.

ports) (Fig. 8; Table 3). Considering that the overall state of fossil preservation was poor to moderate (Table 2), it is possible that the truncation of assemblages due to dissolution and/or reworking may have affected the analyzed interval. In order to solve regional differences in bioevent ages and/or discrepancy between the event ages obtained in this study and the published ages, it is necessary not only to conduct further biostratigraphic studies over a wide geographic range of sites but also to carefully document preservation states of fossils and sedimentary structures in previously analyzed core samples.

3.5 Occurrences of reworked microfossils

During the micropaleontological analysis, occurrences of reworked Miocene taxa and Pliocene marker species were observed. The Miocene diatom taxa include *Denticulopsis ovata* (with a range of ca. 11.1–8.5 Ma; Cody et al., 2008; Tauxe et al., 2012), *Denticulopsis dimorpha* (ca. 12.5–9.8 Ma; Cody et al., 2008; Tauxe et al., 2012), *Denticulopsis dimorpha* var. *areolata* (ca. 10.8–9.7 Ma; Cody et al., 2008), and *Nitzschia denticuloides* (ca. 13.5–11.7 Ma; Cody et al., 2008). The Miocene diatom species were particularly abundant between Samples 113-697B-17X-4, 85–86 cm (172.555 m b.s.f.; 3.73 Ma), and 113-697B-25X-2, 85–86 cm (246.825 m b.s.f., 4.49 Ma), with an abundance peak at 113-697B-21X-1, 85–86 cm (206.755 m b.s.f.; 4.21 Ma) (Fig. 3). In addition, we documented occurrences of *Denticulopsis delicata* that is a middle Miocene to early Pliocene species (ca. 12–4.5 Ma; Cody et al., 2012). The uppermost occurrence of the taxon in Hole 697B coincided with those of other Miocene *Denticulopsis* species (Fig. 3; Table 2), which suggests the taxon could also be reworked. We also observed the occurrence of distinctive fragments of *Siphonosphaera vesuvius*, whose LO occurred at 8.37 Ma

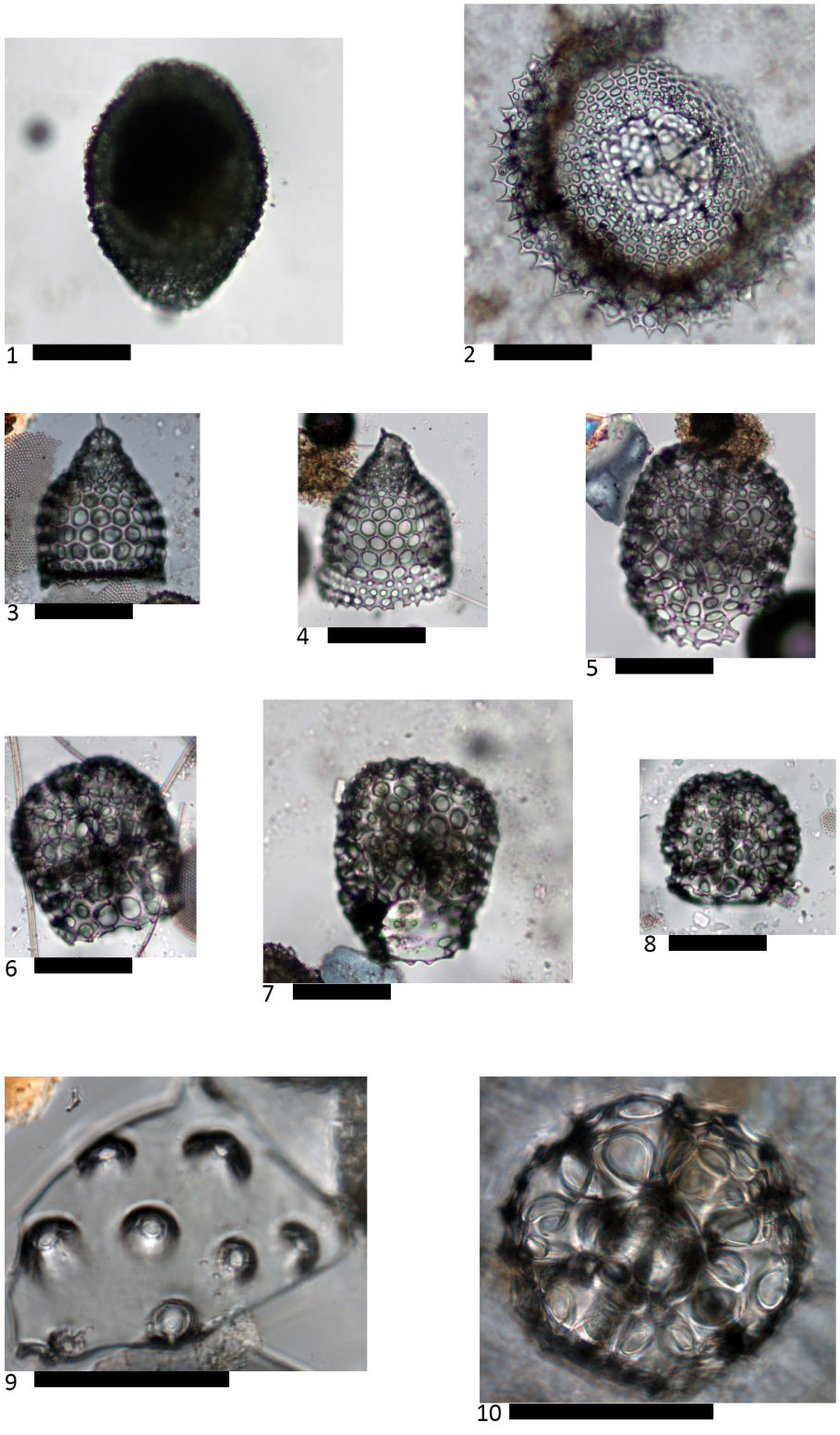

Figure 7. Photomicrographs of selected radiolarian species. **(1)** *Larcopyle polycantha titan* (697B-24X-1, 79–80 cm). **(2)** *Lampromitra coronata* (697B-23X-1, 15–16 cm). **(3)** *Cycladophora pliocenica* (697B-23X-1, 15–16 cm). **(4)** *Cycladophora pliocenica* (697B-21X-1, 85–86 cm). **(5)** *Desmospyris spongiosa* (697B-21X-1, 85–86 cm). **(6)** *Desmospyris spongiosa* (697B-24X-1, 79–80 cm). **(7)** *Desmospyris spongiosa* (697B-14X-4, 85–86 cm). **(8)** *Dendrospyris rhodospyroides* (697B-15X-4, 85–86 cm). **(9)** *Siphonosphaera vesuvius* (697B-21X-1, 85–86 cm). **(10)** *Pseudocubus vema* (697B-14X-2, 85–86 cm). Scale bar: 100 µm.

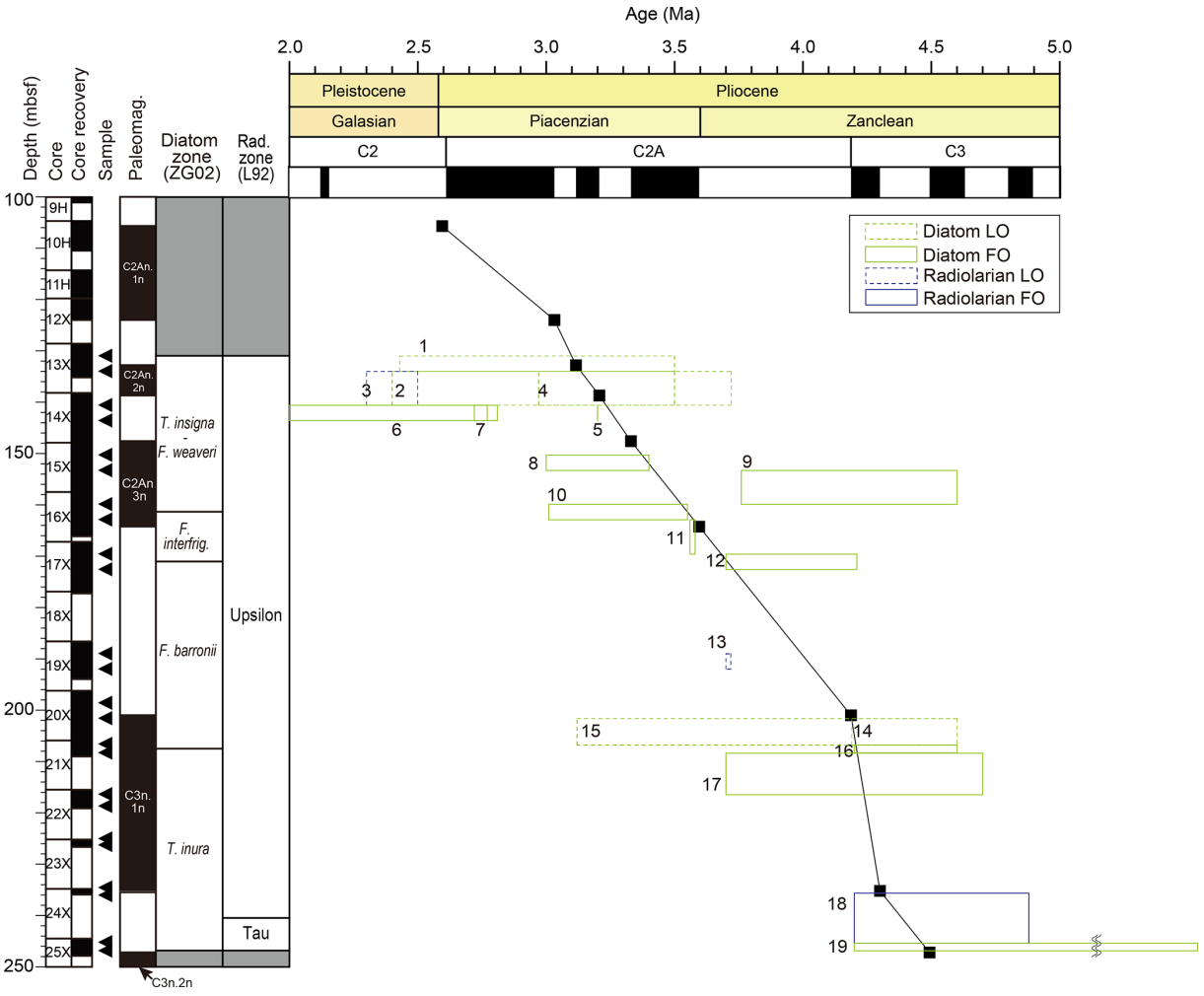

Figure 8. Age–depth plot for Hole 697B. Age ranges of biostratigraphic datums are after previously published ages in the literature shown in Table 3. 1 is for LO of *Thalassiosira complicata*; 2 is for LO of *Thalassiosira striata*; 3 is for LO of *Pseudocubus vema*; 4 is for LO of *Fragilariopsis praeinterfrigidaria*; 5 is for FO of *Fragilariopsis bohatyi*; 6 is for FO of *Rouxia leventerae*; 7 is for FO of *Actinocyclus actinochilus*; 8 is for FO of *Thalassiosira vulnifica*; 9 is for FO of *Thalassiosira lentiginosa*; 10 is for FO of *Fragilariopsis weaveri*' 11 is for FO of *Rhizosolenia harwoodii*; 12 is for FO of *Fragilariopsis interfrigidaria*; 13 is for LO of *Lampromitra coronata*, 14 is for LO of *Fragilariopsis praecurta*; 15 is for LO of *Fragilariopsis aurica*; 16 is for FO of *Fragilariopsis barronii*; 17 is for FO of *Thalassiosira kolbei*; 18 is for FO of *Pseudocubus vema*; and 19 is for FO of *Fragilariopsis praeinterfrigidaria*.

(Florindo et al., 2013) in Sample 113-697B-21X-1, 85–86 cm (206.755 m b.s.f.; 4.21 Ma) (Fig. 7; Table 4).

The abundant reworked Miocene materials in a depth interval of Pliocene age (ca. 4.5 to 3.7 Ma), would be indicative of processes that could have transported these typical Miocene species into Pliocene sediments, e.g., tectonic events (e.g., Civile et al., 2012; Pérez et al., 2019), submarine landslides (e.g., Pérez et al., 2016; Gales et al., 2023), and changes in deep/bottom currents related to fluctuations in the Antarctic Ice Sheet (e.g., Pudsey, 1990; McKay et al., 2012; Lloyd, 2018; O'Connell and Ortiz, 2018). In addition, it is worth noting that marine coastal diatoms, e.g., *Cocconeis* spp., had a similar stratigraphic distribution with *Denticulopsis* species in Site 697 (Fig. 2; Table 2). This may suggest that the adjacent slopes, for example, the South Orkney microcontinent, located to the west of Site 697, could be a potential source of these benthic diatom taxa and the reworked valves from belonging to the genus *Denticulopsis*.

More interestingly, the stratigraphic distribution of *Denticulopsis* species in Hole 697B showed distinct differences between species (Fig. 2; Table 2). Specifically, *Denticulopsis ovata* was relatively abundant in the intervals of between Samples 113-697B-25X-2, 82–83 cm, and 25X-1, 85–86 cm (4.49–4.46 Ma), and between Samples 113-697B-22X-1, 85–86 cm, and 113-697B-21X-1, 85–86 cm (4.24–4.21 Ma), while *Denticulopsis delicata* and *Denticulopsis crassa* were the main components of the *Denticulopsis* species between Samples 113-697B-24X-1, 79–80 cm, and 22X-3, 15–16 cm

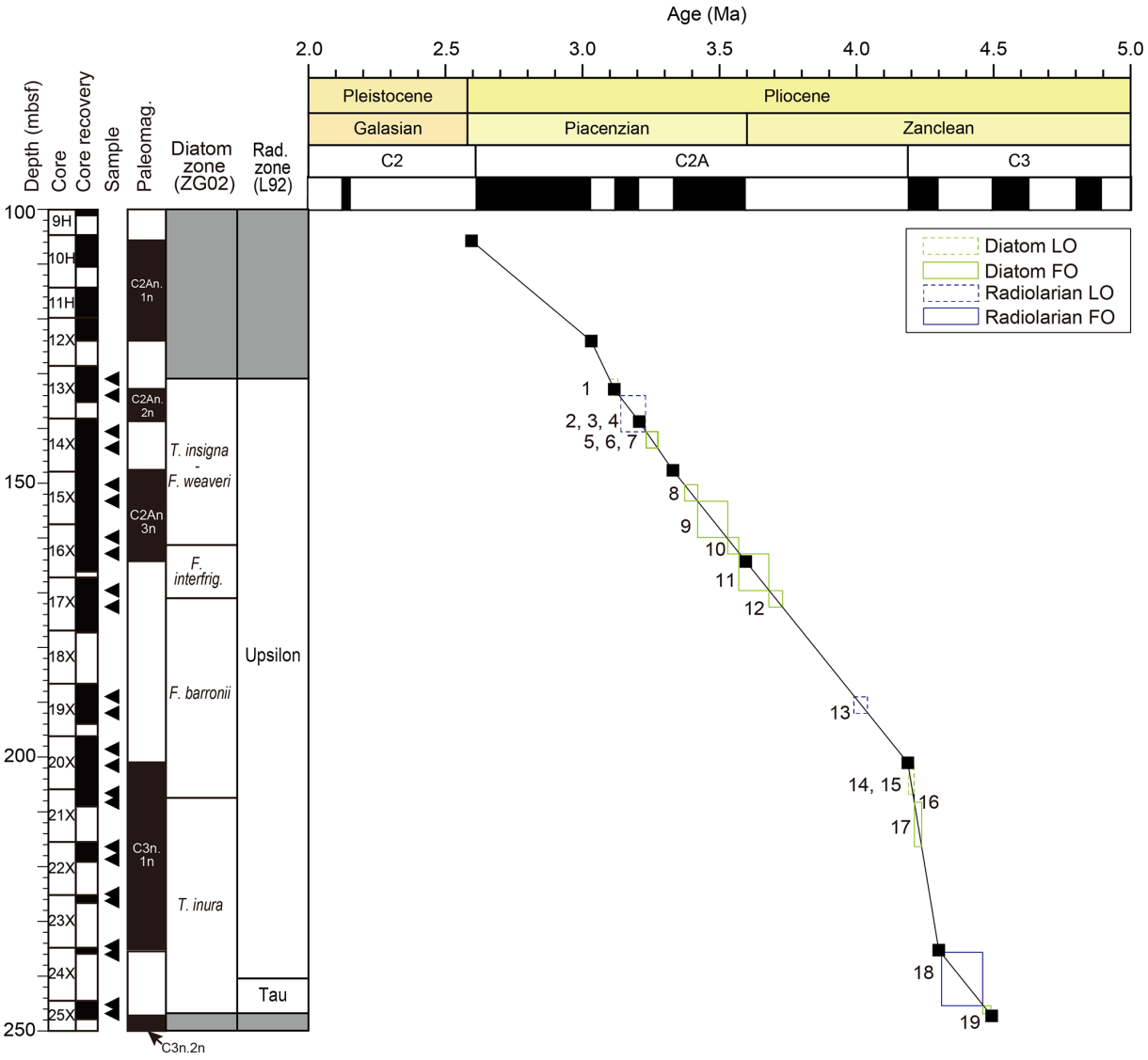

Figure 9. Age–depth plot at Hole 697B. Age ranges of biostratigraphic datums are after the correlation with the paleomagnetic datums in the same sediment core (see Tables 1, 2, and 4). Numbers in the plot indicate each bioevent (see the caption of Fig. 8).

(4.31–4.25 Ma). In an interval between Samples 113-697B-21X-1, 85–86 cm, and 17X-4, 85–86 cm (4.21–3.73 Ma), the "*Denticuliopsis* assemblage" was mainly composed of *Denticulopsis crassa*, *Denticuliopsis delicata*, and *Denticulopsis vulgaris*. The observed distinct intervals for each *Denticulopsis* species would mean that the reworked materials might be derived from source beds of different ages at different intervals. Further research, including the intercorrelation of strata among the surrounding basins by means of seismic profiles, as well as additional micropaleontological analysis of sediment cores (Fig. 1), is needed to discuss the paleoenvironmental significance and regional extent of the Miocene reworked materials found in the early Pliocene interval in the Southern Ocean.

4 Conclusions

The Pliocene epoch is considered a suitable analogue for the Earth's future under the current trend of global warming, and thus, a strong chronological framework of this period is needed, especially for the Antarctic and Southern Ocean regions. We carried out micropaleontological analyses on a section of ODP Leg 113, Hole 697B, located in the Jane Basin in the Atlantic sector of the Southern Ocean in order to improve diatom and radiolarian biostratigraphy of the Pliocene between ca. 4.5–3.1 Ma. As a result, 16 bioevents were observed in the diatom analysis and 3 in the radiolarian analysis (Fig. 9; Table 5). Eight of the diatom events and one radiolarian event were observed for the first time in Hole 697B. These are the LO of *Thalassiosira striata*, FO of *Frag-*

Table 5. Biostratigraphic events identified in this study with calculated ages based on the recent paleomagnetic timescale of Ogg (2020).

Type		Event	Samples (top/bottom samples)	Event depth (m b.s.f.)	Calculated age (Ma)
Diatom	LO	*Thalassiosira complicata*	13X-2, 85–86 cm/13X-4, 85–86 cm	132.455 ± 1.5	3.11 ± 0.01
Diatom	LO	*Thalassiosira striata*	13X-4, 85–86 cm/14X-2, 85–86 cm	137.255 ± 3.3	3.18 ± 0.05
Rad	LO	*Pseudocubus vema*	13X-4, 85–86 cm/14X-2, 85–86 cm	137.255 ± 3.3	3.18 ± 0.05
Diatom	LO	*Fragilariopsis praeinterfrigidaria*	13X-4, 85–86 cm/14X-2, 85–86 cm	137.255 ± 3.3	3.18 ± 0.05
Diatom	FO	*Fragilariopsis bohatyi*	14X-2, 85–86 cm/14X-4, 85–86 cm	142.055 ± 1.5	3.25 ± 0.02
Diatom	FO	*Rouxia leventerae*	14X-2, 85–86 cm/14X-4, 85–86 cm	142.055 ± 1.5	3.25 ± 0.02
Diatom	FO	*Actinocyclus actinochilus*	14X-2, 85–86 cm/14X-4, 85–86 cm	142.055 ± 1.5	3.25 ± 0.02
Diatom	FO	*Thalassiosira vulnifica*	15X-2, 85–86 cm/15X-4, 85–86 cm	151.755 ± 1.5	3.40 ± 0.02
Diatom	FO	*Thalassiosira lentiginosa*	15X-4, 85–86 cm/16X-2, 85–86 cm	156.555 ± 3.3	3.47 ± 0.05
Diatom	FO	*Fragilariopsis weaveri*	16X-2, 85–86 cm/16X-4, 85–86 cm	161.355 ± 1.5	3.55 ± 0.02
Diatom	FO	*Rhizosolenia harwoodii*	16X-4, 85–86 cm/17X-2, 85–86 cm	166.205 ± 3.35	3.63 ± 0.05
Diatom	FO	*Fragilariopsis interfrigidaria*	17X-2, 85–86 cm/17X-4, 85–86 cm	171.055 ± 1.5	3.71 ± 0.02
Rad	LO	*Lampromitra coronata*	19X-2, 85–86 cm/19X-4, 85–86 cm	190.455 ± 1.5	4.02 ± 0.02
Diatom	LO	*Fragilariopsis praecurta*	20X-4, 85–86 cm/21X-1, 85–86 cm	204.155 ± 2.6	4.20 ± 0.01
Diatom	LO	*Fragilariopsis aurica*	20X-4, 85–86 cm/21X-1, 85–86 cm	204.155 ± 2.6	4.20 ± 0.01
Diatom	FO	*Fragilariopsis barronii*	21X-1, 85–86 cm/21X-2, 85–86 cm	207.505 ± 0.75	4.21 ± 0.00
Diatom	FO	*Thalassiosira kolbei*	21X-2, 85–86 cm/22X-1, 85–86 cm	212.305 ± 4.05	4.22 ± 0.01
Rad	FO	*Pseudocubus vema*	24X-1, 85–86 cm/25X-1, 85–86 cm	240.475 ± 4.88	4.38 ± 0.08
Diatom	FO	*Fragilariopsis praeinterfrigidaria*	25X-1, 85–86 cm/25X-2, 82–83 cm	246.09 ± 0.735	4.48 ± 0.01

ilariopsis bohatyi, FO of *Rouxia leventerae*, FO of *Actinocyclus actinochilus*, FO of *Thalassiosira vulnifica*, FO of *Fragilariopsis weaveri*, FO of *Rhizosolenia harwoodii*, FO of *Thalassiosira kolbei*, and LO of *Lampromitra coronata*. The observed bioevents were correlated with the paleomagnetic datums of the same core (Shipboard Scientific Party, 1988) for which the age values were updated according to Ogg (2020). Most of the bioevent ages calculated in this study lay within the age ranges proposed in previous studies (Tables 3 and 5). In addition, the present study allowed the constraining of broad age ranges for some bioevents (Figs. 8 and 9), e.g., FO of *Thalassiosira inura*, FO of *Thalassiosira complicata*, FO of *Fragilariopsis praeinterfrigidaria*, LO of *Fragilariopsis aurica*, FO of *Fragilariopsis interfrigidaria*, LO of *Fragilariopsis praeinterfrigidaria*, LO of *Thalassiosira striata*, LO of *Thalassiosira complicata*, ad FO of *Pseudocubus vema*. The calculated age values obtained for a number of bioevents (e.g., FO of *Thalassiosira lentiginosa* and LO of *Lampromitra coronata*) were not within the previously published age ranges (Tables 3 and 5). Further study is needed, focusing on possible factors such as geographical effects in extinction/appearance ages, truncation of the assemblage due to poor fossil preservation, and reworking.

Abundant reworked Miocene microfossils were identified in ca. 4.5–3.7 Ma sediments, e.g., diatoms such as *Denticulopsis ovata*, *D. crassa*, *D. vulgaris*, *D. dimorpha*, *D. dimorpha* var. *areolata*, *Nitzschia denticuloides*, and a radiolarian *Siphonosphaera vesuvius*. Reworked Miocene sediments embedded on early Pliocene sequences may suggest the disturbance of the sedimentary sequence, perhaps on the adjacent South Orkney microcontinent, which could have been caused by tectonic and/or paleoceanographic events. However, further investigation is needed to address the processes behind such a sedimentary disturbance.

Data availability. Raw data for the diatom and radiolarian analyses are available in Tables 2 and 4, respectively.

Supplement. The supplement related to this article is available online at: https://doi.org/10.5194/jm-43-93-2024-supplement.

Author contributions. This study was designed in a collaboration with YK, IHA, and LFP. YK and IHA carried out diatom and radiolarian analysis, respectively. YK wrote the core of the paper with contributions from IHA and LFP.

Competing interests. The contact author has declared that none of the authors has any competing interests.

Disclaimer. Publisher's note: Copernicus Publications remains neutral with regard to jurisdictional claims made in the text, published maps, institutional affiliations, or any other geographical representation in this paper. While Copernicus Publications makes every effort to include appropriate place names, the final responsibility lies with the authors.

Special issue statement. This article is part of the special issue "Advances in Antarctic chronology, paleoenvironment, and paleoclimate using microfossils: Results from recent coring campaigns". It is not associated with a conference.

Acknowledgements. We appreciate various comments given by the reviewers and the editor, which improved the paper. We would also like to thank all members who contributed to the ODP Leg 113 cruise and the International Ocean Discovery Program's Gulf Coast Repository for sending the samples. This work is supported by KAKENHI (grant nos. 21K14030 and 22H01339), funded by the Japan Society for the Promotion of Science (Yuji Kato), and NERC (grant no. NE/T013648/1; Lara F. Pérez).

Financial support. This research has been supported by the Japan Society for the Promotion of Science (grant nos. 21K14030 and 22H01339) and the Natural Environment Research Council (grant no. NE/T013648/1).

Review statement. This paper was edited by David Harwood and Masao Iwai and reviewed by David Lazarus and one anonymous referee.

References

Akiba, F.: Middle Miocene to Quaternary diatom biostratigraphy in the Nankai Trough and Japan Trench, and modified Lower Miocene through Quaternary diatom zones for middle-to-high latitudes of the North Pacific, in: Initial Reports of the Deep Sea Drilling Project, vol. 87, edited by: Kagami, H., Karig, D. E., Bray, C. J., Charvet, J., Coulbourn, W. T., Kinoshita, H., Lagoe, M. B., Lang, T. H., Lombari, G. A., Lundberg, N., Machihara, T., Mukhopadhyay, P., Smith, A. J., Stein, C. L., Taira, A., Akiba, F., Cadet, J.-P., Fujioka, K., Leggett, J. K., Matsumoto, R., Niitsuma, N., and Whalen, E., U.S. Government Printing Office, Washington D.C., 393–480, https://doi.org/10.2973/dsdp.proc.87.106.1986, 1986.

Amante, C. and Eakins, B. W.: ETOPO1 1 Arc-Minute Global Relief Model: Procedures, Data Sources and Analysis, NOAA Technical Memorandum NESDIS NGDC-24, National Geophysical Data Center, NOAA [data set], https://doi.org/10.7289/V5C8276M, 2009.

Baldauf, J. G. and Barron, J. A.: Diatom biostratigraphy: Kerguelen Plateau and Prydz Bay regions of the Southern Ocean, in: Proceedings of the Ocean Drilling Program, Scientific Results, vol. 119, edited by: Barron, J. A., Larsen, B., Baldauf, J. G., Alibert, C., Berkowitz, S., Caulet, J.-P., Chambers, S. R., Cooper, A. K., Cranston, R. E., Dorn, W. U., Ehrmann, W. U., Fox, R. D., Fryxell, G. A., Hambrey, M. J., Huber, B. T., Jenkins, C. J., Kang, S.-H., Keating, B. H., Mehl, K. W., Noh, I., Ollier, G., Pittenger, A., Sakai, H., Schroder, C. J., Solheim, A., Stockwell, D. A., Thierstein, H. R., Tocher, B., Turner, B. R., Wei, W., Mazzullo, E. K., and Stewart, N. J., College Station, TX (Ocean Drilling Program), 547–598, https://doi.org/10.2973/odp.proc.sr.119.135.1991, 1991.

Berggren, W. A.: Paleogene planktonic foraminifer magnetobiostratigraphy of the southern Kerguelen Plateau (Sites 747–749), in: Proceedings of the Ocean Drilling Program, Scientific Results, vol. 120, edited by: Wise Jr., S. W., Schlich, R., Palmer-Julson, A. A., Aubry, M.-P., Berggren, W. A., Bitschene, P. R., Blackburn, N. A., Breza, J. R., Coffin, M. F., Harwood, D. M., Heider, F., Holmes, M. A., Howard, W. R., Inokuchi, H., Kelts, K., Lazarus, D. B., Mackensen, A., Maruyama, T., Munschy, M., Pratson, E. L., Quilty, P. G., Rack, F., Salters, V. J. M., Sevigny, J. H., Storey, M., Takemura, A., Watkins, D. K., Whitechurch, H., Zachos, J., and Barbu, E. M., College Station, TX (Ocean Drilling Program), 551–568, https://doi.org/10.2973/odp.proc.sr.120.151.1992, 1992a.

Berggren, W. A.: Neogene planktonic foraminifer magnetobiostratigraphy of the southern Kerguelen Plateau (Sites 747, 748, and 751), in: Proceedings of the Ocean Drilling Program, Scientific Results, vol. 120, edited by: Wise Jr., S. W., Schlich, R., Palmer-Julson, A. A., Aubry, M.-P., Berggren, W. A., Bitschene, P. R., Blackburn, N. A., Breza, J. R., Coffin, M. F., Harwood, D. M., Heider, F., Holmes, M. A., Howard, W. R., Inokuchi, H., Kelts, K., Lazarus, D. B., Mackensen, A., Maruyama, T., Munschy, M., Pratson, E. L., Quilty, P. G., Rack, F., Salters, V. J. M., Sevigny, J. H., Storey, M., Takemura, A., Watkins, D. K., Whitechurch, H., Zachos, J., and Barbu, E. M., College Station, TX (Ocean Drilling Program), 631–647, https://doi.org/10.2973/odp.proc.sr.120.153.1992, 1992b.

Berggren, W. A., Kent, D. V., Flynn, J. J., and Van Couvering, J. A.: Cenozoic geochronology, GSA Bulletin, 96, 1407–1418, 1985.

Bohaty, S. M., Wise Jr., S. W., Duncan, R. A., Moore, C. L., and Wallace, P. J.: Neogene diatom biostratigraphy, tephra stratigraphy, and chronology of ODP Hole 1138A, Kerguelen Plateau, in: Proceedings of the Ocean Drilling Program, Scientific Results, vol. 183, edited by: Frey, F. A., Coffin, M. F., Wallace, P. J., and Quilty, P. G., 1–53, https://doi.org/10.2973/odp.proc.sr.183.016.2003, 2003.

Burckle, L. H., Gersonde, R., and Abrams, N.: Late Pliocene-Pleistocene Paleoclimate in the Jane Basin Region ODP Site 697, in: Proceedings of the Ocean Drilling Program, Scientific Results, vol. 113, edited by: Barker, P. F., Kennett, J. P., O'Connell, S., Berkowitz, S.P., Bryant, W. R., Burckle, L. H., Egeberg, P. K., Fuetterer, D. K., Gersonde, R. E., Golovchenko, X., Hamilton, N., Lawver, L. A., Lazarus, D. B., Lonsdale, M. J., Mohr, B. A., Nagao, T., Pereira, C. P. G., Pudsey, C. J., Robert, C. M., Schandl, E. S., Spieß, V., Stott, L. D., Thomas, E., Thompson, K. F. M., Wise Jr., S. W., and Stewart, N. J., College Station, TX (Ocean Drilling Program), 803–809, https://doi.org/10.2973/odp.proc.sr.113.203.1990, 1990.

Cande, S. C. and Kent, D. V.: Revised calibration of the geomagnetic polarity timescale for the Late Cretaceous and Cenozoic, J. Geophys. Res., 100, 6093–6095, 1995.

Caulet, J.-P.: Radiolarians from the Kerguelen Plateau, Leg 119, in: Proceedings of the Ocean Drilling Program, Scientific Results, vol. 119, edited by: Barron, J. A., Larsen, B., Baldauf, J. G., Alibert, C., Berkowitz, S., Caulet, J.-P., Chambers, S. R., Cooper, A. K., Cranston, R. E., Dorn, W. U., Ehrmann, W. U., Fox, R. D., Fryxell, G. A., Hambrey, M. J., Huber, B. T., Jenkins, C. J., Kang, S.-H., Keating, B. H., Mehl, K. W., Noh, I., Ollier, G., Pittenger, A., Sakai, H., Schroder, C. J., Solheim, A., Stockwell, D. A., Thierstein, H. R., Tocher,

B., Turner, B. R., Wei, W., Mazzullo, E. K., and Stewart, N. J., College Station, TX (Ocean Drilling Program), 513–546, https://doi.org/10.2973/odp.proc.sr.119.137.1991, 1991.

Civile, D., Lodolo, E., Vuan, A., and Loreto, M. F.: Tectonics of the Scotia–Antarctica plate boundary constrained from seismic and seismological data, Tectonophysics, 550–553, 17–34, https://doi.org/10.1016/j.tecto.2012.05.002, 2012.

Cody, R. D., Levy, R. H., Harwood, D. M., and Sadler, P. M.: Thinking outside the zone: High-resolution quantitative diatom biochronology for the Antarctic Neogene, Palaeogeogr. Palaeocl., 260, 92–121, 2008.

Cody, R., Levy, R., Crampton, J., Naish, T., Wilson, G., and Harwood, D.: Selection and stability of quantitative stratigraphic age models: Plio-Pleistocene glaciomarine sediments in the ANDRILL 1B drillcore, McMurdo Ice Shelf, Global Planet. Change, 96–97, 143–156, 2012.

Florindo, F., Farmer, R. K., Harwood, D. M., Cody, R. D., Levy, R., Bohaty, S. M., Carter, L., and Winkler, A.: Paleomagnetism and biostratigraphy of sediments from Southern Ocean ODP Site 744 (southern Kerguelen Plateau): Implications for early-to-middle Miocene climate in Antarctica, Global Planet. Change, 110, 434–454, 2013.

Gales, J. A., McKay, R. M., De Santis, L., Rebesco, M., Laberg, J. S., Shevenell, A. E., Harwood, D., Leckie, R. M., Kulhanek, D. K., King, M., Patterson, M., Lucchi, R. G., Kim, S., Kim, S., Dodd, J., Seidenstein, J., Prunella, C., Ferrante, G. M., and IODP Expedition 374 Scientists: Climate-controlled submarine landslides on the Antarctic continental margin, Nat. Commun., 14, 2714, https://doi.org/10.1038/s41467-023-38240-y, 2023.

Gersonde, R. and Bárcena, M. A.: Revision of the upper Pliocene: Pleistocene diatom biostratigraphy for the northern belt of the Southern Ocean, Micropaleontology, 44, 84–98, https://doi.org/10.2307/1486086, 1998.

Gersonde, R. and Burckle, L. H.: Neogene Diatom Biostratigraphy of ODP Leg 113, Weddell Sea (Antarctic Ocean), in: Proceedings of the Ocean Drilling Program, Scientific Results, vol. 113, edited by: Barker, P. F., Kennett, J. P., O'Connell, S., Berkowitz, S. P., Bryant, W. R., Burckle, L. H., Egeberg, P. K., Fuetterer, D. K., Gersonde, R. E., Golovchenko, X., Hamilton, N., Lawver, L. A., Lazarus, D. B., Lonsdale, M. J., Mohr, B. A., Nagao, T., Pereira, C. P. G., Pudsey, C. J., Robert, C. M., Schandl, E. S., Spieß, V., Stott, L. D., Thomas, E., Thompson, K. F. M., Wise Jr., S. W., and Stewart, N. J., College Station, TX (Ocean Drilling Program), 761–789, https://doi.org/10.2973/odp.proc.sr.113.126.1990, 1990.

Gersonde, R., Abelmann, A., Burckle, L. H., Hamilton, N., Lazarus, D., Mccartney, K., O'Brien, P., Spieß, V., and Wise Jr., S. W.: Biostratigraphic synthesis of Neogene siliceous microfossils from the Antarctic ocean, ODP Leg 113 (Weddell Sea), in: Proceedings of the Ocean Drilling Program, Scientific Results, vol. 113, edited by: Barker, P. F., Kennett, J. P., O'Connell, S., Berkowitz, S. P., Bryant, W. R., Burckle, L. H., Egeberg, P. K., Fuetterer, D. K., Gersonde, R. E., Golovchenko, X., Hamilton, N., Lawver, L. A., Lazarus, D. B., Lonsdale, M. J., Mohr, B. A., Nagao, T., Pereira, C. P. G., Pudsey, C. J., Robert, C. M., Schandl, E. S., Spieß, V., Stott, L. D., Thomas, E., Thompson, K. F. M., Wise Jr., S. W., and Stewart, N. J., College Station, TX (Ocean Drilling Program), 915–936, https://doi.org/10.2973/odp.proc.sr.113.209.1990, 1990.

Harwood, D. M. and Maruyama, T.: Middle Eocene to Pleistocene diatom biostratigraphy of Southern Ocean sediments from the Kerguelen Plateau, Leg 120, in: Proceedings of the Ocean Drilling Program, Scientific Results, vol. 120, edited by: Wise Jr., S. W., Schlich, R., Palmer-Julson, A. A., Aubry, M.-P., Berggren, W. A., Bitschene, P. R., Blackburn, N. A., Breza, J. R., Coffin, M. F., Harwood, D. M., Heider, F., Holmes, M. A., Howard, W. R., Inokuchi, H., Kelts, K., Lazarus, D. B., Mackensen, A., Maruyama, T., Munschy, M., Pratson, E. L., Quilty, P. G., Rack, F. R., Salters, V. J. M., Sevigny, J. H., Storey, M., Takemura, A., Watkins, D. K., Whitechurch, H., Zachos, J., and Barbu, E. M., College Station, TX (Ocean Drilling Program), 683–733, https://doi.org/10.2973/odp.proc.sr.120.160.1992, 1992.

Harwood, D. M., Lazarus, D. B., Abelmann, A., Aubry, M.-P., Berggren, W. A., Heider, F., Inokuchi, H., Maruyama, I., McCartney, K., Wei, W., and Wise Jr., S. W.: Neogene integrated magnetobiostratigraphy of the central Kerguelen Plateau, Leg 120, in: Proceedings of the Ocean Drilling Program, Scientific Results, vol. 120, edited by: Wise Jr., S. W., Schlich, R., Palmer-Julson, A. A., Aubry, M.-P., Berggren, W. A., Bitschene, P. R., Blackburn, N. A., Breza, J. R., Coffin, M. F., Harwood, D. M., Heider, F., Holmes, M. A., Howard, W. R., Inokuchi, H., Kelts, K., Lazarus, D. B., Mackensen, A., Maruyama, T., Munschy, M., Pratson, E. L., Quilty, P. G., Rack, F. R., Salters, V. J. M., Sevigny, J. H., Storey, M., Takemura, A., Watkins, D. K., Whitechurch, H., Zachos, J., and Barbu, E. M., College Station, TX (Ocean Drilling Program), 1031–1052, https://doi.org/10.2973/odp.proc.sr.120.185.1992, 1992.

Iwai, M. and Winter, D.: Data report: taxonomic notes of Neogene diatoms from the western Antarctic peninsula: Ocean Drilling Program Leg 178, in: Proceedings of the Ocean Drilling Program, Scientific Results, vol. 178, edited by: Barker, P. F., Camerlenghi, A., Acton, G. D., and Ramsay, A. T. S., College Station, TX (Ocean Drilling Program), 1–57, https://doi.org/10.2973/odp.proc.sr.178.239.2002, 2002.

Iwai, M., Acton, G. D., Lazarus, D., Osterman, L. E., and Williams, T.: Magnetobiochronologic synthesis of ODP Leg 178 rise sediments from the Pacific sector of the Southern Ocean: Sites 1095, 1096, and 1101, in: Proceedings of the Ocean Drilling Program, Scientific Results, vol. 178, edited by: Barker, P. F., Camerlenghi, A., Acton, G. D., and Ramsay, A. T. S., College Station, TX (Ocean Drilling Program), 1–40, https://doi.org/10.2973/odp.proc.sr.178.236.2002, 2002.

Jordan, R. W. and Priddle, J.: Fossil members of the diatom genus *Proboscia*, Diatom Res., 6, 55–61, https://doi.org/10.1080/0269249X.1991.9705147, 1991.

Kennett, J. P. and Barker, P. F.: Latest Cretaceous to Cenozoic climate and oceanographic developments in the Weddell Sea, Antarctica: an ocean-drilling perspective, in: Proceedings of the Ocean Drilling Program, Scientific Results, vol. 113, edited by: Barker, P. F., Kennett, J. P., O'Connell, S., Berkowitz, S. P., Bryant, W. R., Burckle, L. H., Egeberg, P. K., Fuetterer, D. K., Gersonde, R. E., Golovchenko, X., Hamilton, N., Lawver, L. A., Lazarus, D. B., Lonsdale, M. J., Mohr, B. A., Nagao, T., Pereira, C. P. G., Pudsey, C. J., Robert, C. M., Schandl, E. S., Spieß, V., Stott, L. D., Thomas, E., Thompson, K. F. M., Wise Jr., S. W., and Stewart, N. J., College Station, TX (Ocean Drilling Program), 937–960, https://doi.org/10.2973/odp.proc.sr.113.195.1990, 1990.

Lazarus, D.: Middle Miocene to Recent Radiolarians from the Weddell Sea, Antarctica, ODP Leg 113, in: Proceedings of the Ocean Drilling Program, Scientific Results, vol. 113, edited by: Barker, P. F., Kennett, J. P., O'Connell, S., Berkowitz, S. P., Bryant, W. R., Burckle, L. H., Egeberg, P. K., Fuetterer, D. K., Gersonde, R. E., Golovchenko, X., Hamilton, N., Lawver, L. A., Lazarus, D. B., Lonsdale, M. J., Mohr, B. A., Nagao, T., Pereira, C. P. G., Pudsey, C. J., Robert, C.M., Schandl, E. S., Spieß, V., Stott, L. D., Thomas, E., Thompson, K. F. M., Wise Jr., S. W., and Stewart, N. J., College Station, TX (Ocean Drilling Program), 709–727, https://doi.org/10.2973/odp.proc.sr.113.132.1990, 1990.

Lazarus, D.: Antarctic Neogene radiolarians from the Kerguelen Plateau, Legs 119 and 120, in: Proceedings of the Ocean Drilling Program, Scientific Results, vol. 120, edited by: Wise, S. W., Jr., Schlich, R., Palmer-Julson, A. A., Aubry, M.-P., Berggren, W. A., Bitschene, P. R., Blackburn, N. A., Breza, J. R., Coffin, M. F., Harwood, D. M., Heider, F., Holmes, M. A., Howard, W. R., Inokuchi, H., Kelts, K., Lazarus, D. B., Mackensen, A., Maruyama, T., Munschy, M., Pratson, E. L., Quilty, P. G., Rack, F. R., Salters, V. J. M., Sevigny, J. H., Storey, M., Takemura, A., Watkins, D. K., Whitechurch, H., Zachos, J., and Barbu, E. M., College Station, TX (Ocean Drilling Program), 785–802, https://doi.org/10.2973/odp.proc.sr.120.192.1992, 1992.

Lazarus, D. B.: Late Miocene to early Pliocene radiolarians from glaciomarine drift deposits, ODP Leg 178, Hole 1095B (Bellinghausen Basin, Antarctic Ocean), in: Proceedings of the Ocean Drilling Program, Scientific Results, vol. 178, edited by: Barker, P. F., Camerlenghi, A., Acton, G. D., and Ramsay, A. T. S., College Station, TX (Ocean Drilling Program), 1–22, https://doi.org/10.2973/odp.proc.sr.178.218.2001, 2001.

Lazarus, D.: Environmental control of diversity, evolutionary rates and taxa longevities in Antarctic Neogene radiolaria, Palaeontol. Electron., 5, 1–32, 2002.

Lloyd, F. W.: Zanclean (early Pliocene) sediment records of ice-sheet instability at ODP Site 697 (Jane Basin), NW Weddell Sea, South Orkney microcontinent. Learning Science Through Research, Short Contributions, Keck Geology Consortium, 31, 1–7, https://doi.org/10.18277/AKRSG.2019.31.24, 2018.

McCollum, D. W.: Diatom stratigraphy of the Southern Ocean, in: Initial Reports of the Deep Sea Drilling Project, vol. 28, edited by: Hayes, D. E., Frakes, L. A., Barrett, P. J., Burns, D. A., Chen, P.-H., Ford, A. B., Kaneps, A. G., Kemp, E. M., McCollum, D. W., Piper, D. J. W., Wall, R. E., and Webb, P. N., U.S. Government Printing Office, Washington D.C., 515–571, https://doi.org/10.2973/dsdp.proc.28.112.1975, 1975.

McKay, R., Naish, T., Carter, L., Riesselman, C., Dunbar, R., Sjunneskog, C., Winter, D., Sangiorgi, F., Warren, C., Pagani, M., Schouten, S., Willmott, V., Levy, R., DeConto, R., and Powell, R. D.: Antarctic and Southern Ocean influences on Late Pliocene global cooling, P. Natl. Acad. Sci. USA, 109, 6423–6428, https://doi.org/10.1073/pnas.1112248109, 2012.

Mutterlose, J. and Wise Jr., S. W.: Lower Cretaceous nannofossil biostratigraphy of ODP Leg 113 Holes 692B and 693A, continental slope off East Antarctica, Weddell Sea. in: Proceedings of the Ocean Drilling Program, Scientific Results, vol. 113, edited by: Barker, P. F., Kennett, J. P., O'Connell, S., Berkowitz, S. P., Bryant, W. R., Burckle, L. H., Egeberg, P. K., Fuetterer, D. K., Gersonde, R. E., Golovchenko, X., Hamilton, N., Lawver, L. A., Lazarus, D. B., Lonsdale, M. J., Mohr, B. A., Nagao, T., Pereira, C. P. G., Pudsey, C. J., Robert, C. M., Schandl, E. S., Spieß, V., Stott, L. D., Thomas, E., Thompson, K. F. M., Wise Jr., S. W., and Stewart, N. J., College Station, TX (Ocean Drilling Program), 325–351, https://doi.org/10.2973/odp.proc.sr.113.143.1990, 1990.

O'Connell, S. and Ortiz, J.: Multiple Proxies for Investigating Glacial History of Antarctica From ODP Sites 696 & 697. Learning Science Through Research, Short Contributions, Keck Geology Consortium, 31, 1–6, https://doi.org/10.18277/AKRSG.2019.31.20, 2018.

Ogg, J. G.: Geomagnetic polarity time scale, in: Geologic Time Scale 2020 edited by: Gradstein, F. M., Ogg, J. G., Schmitz, M. D., and Ogg, G. M., Elsevier, Amsterdam, Oxford, Cambridge, 159–192, 2020.

Orsi, A. H., Whitworth, T., and Nowlin, W. D.: On the meridional extent and fronts of the Antarctic Circumpolar Current, Deep-Sea Res., 42, 641–673, https://doi.org/10.1016/0967-0637(95)00021-W, 1995.

Pérez, L. F., Bohoyo, F., Hernández-Molina, F. J., Casas, D., Galindo-Zaldívar, J., Ruano, P., and Maldonado, A.: Tectonic activity evolution of the Scotia-Antarctic Plate boundary from mass transport deposit analysis, J. Geophys. Res.-Sol. Ea., 121, 2216–2234, https://doi.org/10.1002/2015JB012622, 2016.

Pérez, L. F., Henández-Molina, F. J., Lodolo, E., Bohoyo, F., Galindo-Zaldívar, J., and Maldonado, A.: Oceanographic and climatic consequences of the tectonic evolution of the southern scotia sea basins, Antarctica, Earth-Sci. Rev., 198, 102922, https://doi.org/10.1016/j.earscirev.2019.102922, 2019.

Pospichal, J. J. and Wise Jr., S. W.: Maestrichtian calcareous nannofossil biostratigraphy of Maud Rise, ODP Leg 113 Sites 689 and 690, Weddell Sea, in: Proceedings of the Ocean Drilling Program, Scientific Results, vol. 113, edited by: Barker, P. F., Kennett, J. P., O'Connell, S., Berkowitz, S. P., Bryant, W. R., Burckle, L. H., Egeberg, P. K., Fuetterer, D. K., Gersonde, R. E., Golovchenko, X., Hamilton, N., Lawver, L. A., Lazarus, D. B., Lonsdale, M. J., Mohr, B. A., Nagao, T., Pereira, C. P. G., Pudsey, C. J., Robert, C. M., Schandl, E. S., Spieß, V., Stott, L. D., Thomas, E., Thompson, K. F. M., Wise Jr., S. W., and Stewart, N. J., College Station, TX (Ocean Drilling Program), 465–487, https://doi.org/10.2973/odp.proc.sr.113.124.1990, 1990.

Pudsey, C. J.: Grain Size and Diatom Content of Hemipelagic Sediments at Site 697, ODP Leg 113: A Record of Pliocene-Pleistocene Climate, in: Proceedings of the Ocean Drilling Program, Scientific Results, vol. 113, edited by: Barker, P. F., Kennett, J. P., O'Connell, S., Berkowitz, S. P., Bryant, W. R., Burckle, L.H., Egeberg, P. K., Fuetterer, D. K., Gersonde, R. E., Golovchenko, X., Hamilton, N., Lawver, L. A., Lazarus, D. B., Lonsdale, M. J., Mohr, B. A., Nagao, T., Pereira, C. P. G., Pudsey, C. J., Robert, C. M., Schandl, E. S., Spieß, V., Stott, L. D., Thomas, E., Thompson, K. F. M., Wise Jr., S. W., and Stewart, N. J., Ocean Drilling Program, College Station, TX, 111–120, https://doi.org/10.2973/odp.proc.sr.113.147.1990, 1990.

Ramsay, A. T. S. and Baldauf, J. G.: A reassessment of the Southern Ocean biochronology, Kluwer, London, Memoir No. 18 of Geological Society of London, ISBN 1-86239-027-4, ISBN 978-1-86239-027-0, 1999.

Saavedra-Pellitero, M., Baumann, K.-H., Ullermann, J., and Lamy, F.: Marine Isotope Stage 11 in the Pacific sector of the Southern

Ocean; a coccolithophore perspective, Quaternary Sci. Rev., 158, 1–14, https://doi.org/10.1016/j.quascirev.2016.12.020, 2017.

Scherer, R. P., Gladenkov, A. Y., and Barron, J. A.: Methods and applications of Cenozoic marine diatom biostratigraphy, The Paleontological Society Papers, 13, 61–83, https://doi.org/10.1017/S1089332600001467, 2007.

Shipboard Scientific Party: Site 697, in: Proc. ODP, Init. Repts., 113, edited by: Barker, P. F., Kennett, J. P., O'Connell, S., Berkowitz, S. P., Bryant, W. R., Burckle, L. H., Egeberg, P. K., Fuetterer, D. K., Gersonde, R. E., Golovchenko, X., Hamilton, N., Lawver, L. A., Lazarus, D. B., Lonsdale, M. J., Mohr, B. A., Nagao, T., Pereira, C. P. G., Pudsey, C. J., Robert, C. M., Schandl, E. S., Spieß, V., Stott, L. D., Thomas, E., Thompson, K. F. M., Wise Jr., S. W., and Stewart, N. J., College Station, TX (Ocean Drilling Program), 705–774, https://doi.org/10.2973/odp.proc.ir.113.113.1988, 1988.

Sjunneskog, C., Riesselman, C., Winter, D., and Scherer, R.: Fragilariopsis diatom evolution in Pliocene and Pleistocene Antarctic shelf sediments, Micropaleontology, 58, 273–289, 2012.

Tauxe, L., Stickley, C. E., Sugisaki, S., Bijl, P. K., Bohaty, S. M., Brinkhuis, H., Escutia, C., Flores, J. A., Houben, A. J. P., Iwai, M., Jiménez-Espejo, F., McKay, R., Passchier, S., Pross, J., Riesselman, C. R., Röhl, U., Sangiorgi, F., Welsh, K., Klaus, A., Fehr, A., Bendle, J. A. P., Dunbar, R., Gonzàlez, J., Hayden, T., Katsuki, K., Olney, M. P., Pekar, S. F., Shrivastava, P. K., van de Flierdt, T., Williams, T., and Yamane, M.: Chronostratigraphic framework for the IODP Expedition 318 cores from the Wilkes Land Margin: Constraints for paleoceanographic reconstruction, Paleoceanography, 27, PA2214, https://doi.org/10.1029/2012pa002308, 2012.

Tetard, M., Marchant, R., Cortese, G., Gally, Y., de Garidel-Thoron, T., and Beaufort, L.: Technical note: A new automated radiolarian image acquisition, stacking, processing, segmentation and identification workflow, Clim. Past, 16, 2415–2429, https://doi.org/10.5194/cp-16-2415-2020, 2020.

Vigour, R. and Lazarus, D.: Biostratigraphy of late Miocene-early Pliocene radiolarians from ODP Leg 183 Site 1381, in: Proceedings of the Ocean Drilling Program, Scientific Results, vol. 183, edited by: Frey, F. A., Coffin, M. F., Wallace, P. J., and Quilty, P. G., College Station, TX (Ocean Drilling Program), 1–17, https://doi.org/10.2973/odp.proc.sr.183.007.2002, 2002.

Weaver, F. M. and Gombos Jr., A. M.: Southern high-latitude diatom biostratigraphy, in: The Deep Sea Drilling Project: A Decade of Progress, vol. 32, edited by: Warme, J. E., Douglas, R. G., and Winterer, E. L., SEPM Society for Sedimentary Geology, 445–470, https://doi.org/10.2110/pec.81.32.0445, 1981.

Winter, D. and Iwai, M.: Data report: Neogene diatom biostratigraphy, Antarctic Peninsula Pacific margin, ODP Leg 178 rise sites, in: Proceedings of the Ocean Drilling Program, Scientific Results, vol. 178, edited by: Barker, P. F., Camerlenghi, A., Acton, G. D., and Ramsay, A. T. S., College Station, TX (Ocean Drilling Program), 1–25., https://doi.org/10.2973/odp.proc.sr.178.230.2002, 2002.

Winter, D., Sjunneskog, C., Scherer, R., Maffioli, P., Riesselman, C., and Harwood, D.: Pliocene–Pleistocene diatom biostratigraphy of nearshore Antarctica from the AND-1B drillcore, McMurdo Sound, Global Planet. Change, 96–97, 59–74, https://doi.org/10.1016/j.gloplacha.2010.04.004, 2012.

Yanagisawa, Y. and Akiba, F.: Taxonomy and phylogeny of the three marine diatom genera, *Crucidenticula, Denticulopsis* and *Neodenticula*, Bulletin of the Geological Survey of Japan, 41, 197–301, 1990.

Zielinski, U. and Gersonde, R.: Plio-Pleistocene diatom biostratigraphy from ODP Leg 177, Atlantic sector of the Southern Ocean, Mar. Micropaleontol., 45, 225–268, https://doi.org/10.1016/S0377-8398(02)00031-2, 2002.